ARTICLE

The Genomics of Arthrogryposis, a Complex Trait: Candidate Genes and Further Evidence for Oligogenic Inheritance

Davut Pehlivan,[1,2,28] Yavuz Bayram,[1,3,28] Nilay Gunes,[4] Zeynep Coban Akdemir,[1] Anju Shukla,[5] Tatjana Bierhals,[6] Burcu Tabakci,[7] Yavuz Sahin,[8] Alper Gezdirici,[9] Jawid M. Fatih,[1] Elif Yilmaz Gulec,[9] Gozde Yesil,[10] Jaya Punetha,[1] Zeynep Ocak,[9] Christopher M. Grochowski,[1] Ender Karaca,[1] Hatice Mutlu Albayrak,[11] Periyasamy Radhakrishnan,[5] Haktan Bagis Erdem,[12] Ibrahim Sahin,[13] Timur Yildirim,[14] Ilhan A. Bayhan,[14] Aysegul Bursali,[14] Muhsin Elmas,[15] Zafer Yuksel,[16] Ozturk Ozdemir,[17] Fatma Silan,[17] Onur Yildiz,[17] Osman Yesilbas,[18] Sedat Isikay,[19] Burhan Balta,[20] Shen Gu,[1] Shalini N. Jhangiani,[21] Harsha Doddapaneni,[21] Jianhong Hu,[21] Donna M. Muzny,[21] Baylor-Hopkins Center for Mendelian Genomics, Eric Boerwinkle,[21,22] Richard A. Gibbs,[1,21] Konstantinos Tsiakas,[23] Maja Hempel,[6] Katta Mohan Girisha,[5] Davut Gul,[24] Jennifer E. Posey,[1] Nursel H. Elcioglu,[7,25] Beyhan Tuysuz,[4] and James R. Lupski[1,21,26,27,*]

Arthrogryposis is a clinical finding that is present either as a feature of a neuromuscular condition or as part of a systemic disease in over 400 Mendelian conditions. The underlying molecular etiology remains largely unknown because of genetic and phenotypic heterogeneity. We applied exome sequencing (ES) in a cohort of 89 families with the clinical sign of arthrogryposis. Additional molecular techniques including array comparative genomic hybridization (aCGH) and Droplet Digital PCR (ddPCR) were performed on individuals who were found to have pathogenic copy number variants (CNVs) and mosaicism, respectively. A molecular diagnosis was established in 65.2% (58/89) of families. Eleven out of 58 families (19.0%) showed evidence for potential involvement of pathogenic variation at more than one locus, probably driven by absence of heterozygosity (AOH) burden due to identity-by-descent (IBD). *RYR3*, *MYOM2*, *ERGIC1*, *SPTBN4*, and *ABCA7* represent genes, identified in two or more families, for which mutations are probably causative for arthrogryposis. We also provide evidence for the involvement of CNVs in the etiology of arthrogryposis and for the idea that both mono-allelic and bi-allelic variants in the same gene cause either similar or distinct syndromes. We were able to identify the molecular etiology in nine out of 20 families who underwent reanalysis. In summary, our data from family-based ES further delineate the molecular etiology of arthrogryposis, yielded several candidate disease-associated genes, and provide evidence for mutational burden in a biological pathway or network. Our study also highlights the importance of reanalysis of individuals with unsolved diagnoses in conjunction with sequencing extended family members.

Introduction

Arthrogryposis is a term that describes the clinical observation of joint contractures in more than one segment of the body. It does not describe a specific disease entity, but rather represents a descriptive clinical neuromuscular sign for multiple contractures associated with different medical conditions. The primary underlying cause of arthrogryposis is postulated to be decreased fetal joint mobility during intrauterine development. Lack of fetal joint mobility might result from multiple etiologies for perturbed neuromuscular function; these etiologies include intrinsic causes

[1]Department of Molecular and Human Genetics, Baylor College of Medicine, Houston, TX 77030, USA; [2]Section of Pediatric Neurology and Developmental Neuroscience, Department of Pediatrics, Baylor College of Medicine, Houston, TX 77030, USA; [3]Department of Genetics and Genomic Sciences, Icahn School of Medicine at Mount Sinai, New York, NY 10029, USA; [4]Department of Pediatric Genetics, Istanbul University-Cerrahpasa Medical Faculty, Istanbul 34096, Turkey; [5]Department of Medical Genetics, Kasturba Medical College, Manipal, Manipal Academy of Higher Education, Manipal 576104, India; [6]Institute of Human Genetics, University Medical Center Hamburg-Eppendorf, Martinistraße 52, Hamburg 20246, Germany; [7]Department of Pediatric Genetics, Marmara University Medical School, Istanbul 34854, Turkey; [8]Department of Medical Genetics, Necip Fazıl City Hospital, Kahramanmaras 46050, Turkey; [9]Department of Medical Genetics, Kanuni Sultan Suleyman Training and Research Hospital, Istanbul 34303, Turkey; [10]Department of Medical Genetics, Bezmi Alem Vakif University Faculty of Medicine, Istanbul 34093, Turkey; [11]Department of Pediatrics, Division of Pediatric Genetics, Faculty of Medicine, Ondokuz Mayıs University, Samsun 55270, Turkey; [12]Department of Medical Genetics, University of Health Sciences, Diskapi Yildirim Beyazit Training and Research Hospital, Ankara 06110, Turkey; [13]Department of Medical Genetics, University of Erzurum, School of Medicine, Erzurum 25240, Turkey; [14]Department of Orthopedics and Traumatology, Baltalimani Bone Diseases Training and Research Hospital, Istanbul 34470, Turkey; [15]Department of Medical Genetics, Afyon Kocatepe University, School of Medicine, Afyon 03218, Turkey; [16]Medical Genetics Clinic, Mersin Women and Children Hospital, Mersin 33330, Turkey; [17]Department of Medical Genetics, Faculty of Medicine, Onsekiz Mart University, Canakkale 17000, Turkey; [18]Division of Critical Care Medicine, Department of Pediatrics, University of Health Sciences, Van Training and Research Hospital, Van 65130, Turkey; [19]Department of Physiotherapy and Rehabilitation, Hasan Kalyoncu University, School of Health Sciences, Gaziantep 27000, Turkey; [20]Department of Medical Genetics, Kayseri Training and Research Hospital, Kayseri 38080, Turkey; [21]Human Genome Sequencing Center, Baylor College of Medicine, Houston, TX 77030, USA; [22]Human Genetics Center, University of Texas Health Science Center at Houston School of Public Health, Houston, TX, USA; [23]Department of Pediatrics, University Medical Center Hamburg-Eppendorf, Hamburg, 20246, Germany; [24]Department of Medical Genetics, Gulhane Military Medical School, Ankara 06010, Turkey; [25]Eastern Mediterranean University School of Medicine, Cyprus, Mersin 10, Turkey; [26]Department of Pediatrics, Baylor College of Medicine, Houston, TX 77030, USA; [27]Texas Children's Hospital, Houston, TX 77030, USA
[28]These authors contributed equally to this work
*Correspondence: jlupski@bcm.edu
https://doi.org/10.1016/j.ajhg.2019.05.015.

A

Study group	Number of families
Phase I	**48**
Solved	28
Unsolved	20
Phase II	**89**
Newly recruited	69
Unsolved from Phase I expanded to trio ES	10
Unsolved from Phase I reanalyzed	10
GeneMatcher	**2**
Total	**119**

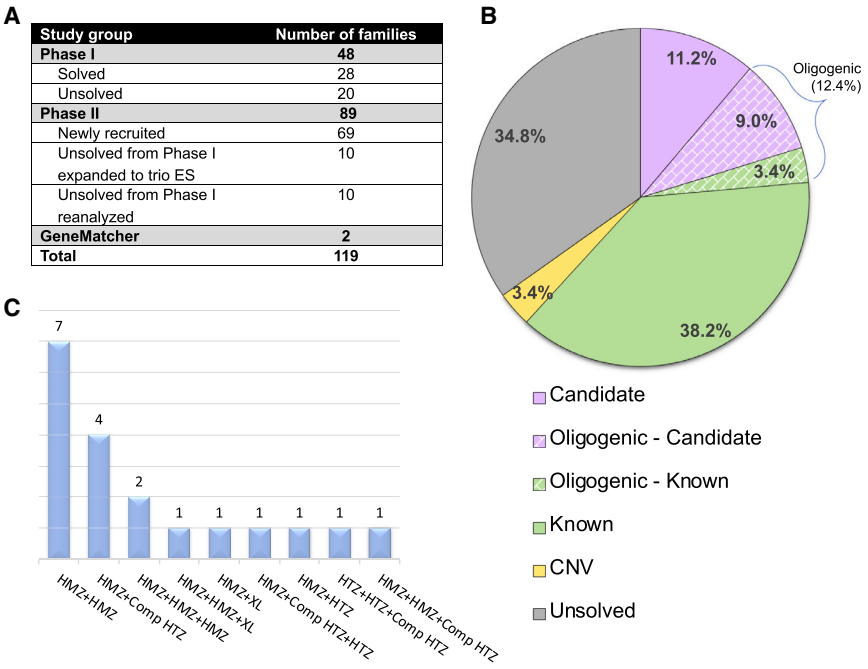

Figure 1. Distribution and Molecular Results of Enrolled Individuals in the Arthrogryposis Cohort and Families with Multilocus Pathogenic Variation

(A) Distribution of individuals enrolled in arthrogryposis cohort.

(B) A pie chart displaying the distribution of molecular findings for each individual in this study (i.e., phase II) of the arthrogryposis cohort (89 families). Multilocus pathogenic variant model families were classified according to muscle gene status. A corresponding explanation for the colors in the pie chart is below the chart. The abbreviation CNV = copy number variation.

(C) Families affected with multilocus pathogenic variation (19 families) from phase I + II. Abbreviations are as follows: HMZ = homozygous, HTZ = heterozygous, Comp HTZ = compound heterozygous, and XL = hemizygous male.

such as neurological disorders, muscle diseases, skeletal conditions, and abnormalities in connective and cartilage tissue and extrinsic factors such as maternal diseases, intrauterine space limitations, maternal exposures to drugs or chemicals, and decreased blood supply to the fetus.[1] Thus, arthrogryposis can be thought of as a birth defect due to a malformation in some individuals and as a deformation in others or, also, as a complex trait with both genetic and environmental influences.

The prevalence of arthrogryposis ranges from ~1/3000–5000, and it has a high (~50%) mortality rate.[2] The etiology is thought to be mostly genetic, and variants in more than 300 genes associated with over 400 Mendelian conditions have been identified.[3] Copy number variants (CNVs) including microdeletions and duplications have also been implicated in individuals with arthrogryposis.[4–7] The molecular etiology of arthrogryposis and the potential biological pathways involved remain unknown in many individuals; molecular diagnostic rates of 47% in an Australian cohort of 38 families and 58% in a Turkish cohort of 48 families (phase I of this study) have been reported.[8,9] One of the insights into the potential genetic architecture and underlying genetic etiology of some individuals with arthrogryposis, recognized only through genome-wide screening of coding regions, is the contribution of rare variants in multiple loci of a single personal genome to the observed phenotype (i.e., multiple molecular diagnoses leading to a blended phenotype).[10–14] Additionally, both mono- and bi-allelic variants of several genes, responsible respectively for autosomal-dominant (AD) and autosomal-recessive (AR) disease traits, are known to cause either the same or a different syndrome and are being reported more frequently with genome-wide analysis techniques such as exome sequencing (ES).[8,15–19]

We previously reported molecular findings from 28 out of 48 arthrogryposis-affected families (a molecular diagnostic yield of 58.3%).[8] In the current study, we enrolled an additional 71 families (including two families found through GeneMatcher) and performed a reanalysis of 20 undiagnosed families, including ten families for which the initial proband-exome was extended to trio exome with parental samples, from the previously reported cohort. We provide clinical and genomic evidence for 15 candidate arthrogryposis-associated genes and four candidate developmental delay and intellectual disability (DD and ID)-associated genes. Our findings suggest mutational burden might contribute to the molecular diagnosis of some individuals with arthrogryposis through the aggregation of multilocus pathogenic variation in a personal genome.

Material and Methods

Study Participants

We recruited 103 individuals and fetuses from 91 mostly Turkish families (only two families of different ethnicity were found through GeneMatcher) with the presenting clinical feature of arthrogryposis (Figure 1A). Of the 103 participants, 53 were female (51.5%), 47 were male (45.6%), and three (2.9%) had a gender that was not reported (fetus). Ages ranged from 19 gestational weeks to 42 years old. Thirty-four of the participant families were characterized as having syndromic arthrogryposis, whereas 57 had an apparent isolated neuromuscular disorder. Parental consanguinity was reported in 46 families (50.5%), and 45 families (49.5%) had no historical evidence for parental consanguinity. After all relevant family members provided written informed consent, peripheral blood was collected from affected individuals, parents, and unaffected relatives if available. Genomic DNA was extracted from blood leukocytes according to standard procedures. All genomic studies were performed on DNA samples isolated from blood. This study was approved by the institutional review board at Baylor College of Medicine (IRB protocol # H-29697).

Exome Sequencing

We applied ES to selected family members through the Baylor-Hopkins Center for Mendelian Genomics (BHCMG) research initiative.[20] All experimental procedures were performed according to previously described methods.[21] Briefly, genomic DNA samples underwent exome capture with Baylor College of Medicine Human Genome Sequencing Center core design (52 Mb, Roche NimbleGen, RRID: nif-0000-31466), and were then sequenced on the HiSeq platform (Illumina) with ~100× depth of coverage. Sequence data were aligned and mapped to the human genome reference sequence (hg19) with the Mercury in-house bioinformatics pipeline.[22] Variants were called with ATLAS2 (an integrative variant analysis pipeline optimized for variant discovery) and SAMTOOLS (RRID: nlx_154607; the Sequence Alignment/Map) suites, and they were annotated with an in-house-developed annotation pipeline that uses annotation of genetic variants and additional tools and databases.[23–25] Variant filtering parsed nonsynonymous variants by population frequency data. The minor allele frequency of candidate variants was obtained from publicly available databases such as the 1000 Genomes Project and other large-scale exome-sequencing projects, including the Exome Variant Server; the National Heart, Lung, and Blood Institute (NHLBI) Grand Opportunity Exome Sequencing Project (ESP); the Atherosclerosis Risk in Communities Study Database (ARIC); the Genome Aggregation Database (gnomAD); the Exome Aggregation Consortium (ExAC); and our in-house-generated exome database (~13,000 individuals) at the Baylor College of Medicine Human Genome Sequencing Center.

In order to detect disease-causing single nucleotide variants (SNVs), a stepwise analysis workflow was implemented.[26] To be able to identify CNVs, we used publicly available bioinformatics tools, including XHMM (eXome-Hidden Markov Model), CoNIFER, and CoNVex programs, for larger CNVs (≥3 exon deletion and duplication), and we used an in-house-developed software, HMZDelFinder, for smaller homozygous and hemizygous intragenic CNVs.[27,28] In order to capture *de novo* disease-causing variants, we used another in-house-developed program called DNM (*de novo* mutation)-Finder.[26] All candidate genes were submitted to GeneMatcher to identify additional individuals with variants likely to be damaging in the same gene.[29,30] To examine absence of heterozygosity (AOH) regions, which might represent identity-by-descent (IBD), surrounding candidate variants, we calculated B-allele frequency by using exome variant data as a ratio of variant reads to total reads.[31] These data were then processed with the circular binary segmentation (CBS) algorithm[32] in order to identify AOH regions. The calculated AOH intervals from BafCalculator could represent "apparent genetic transmission distortion" of individual genomic loci, resulting in runs-of-homozygosity (ROHs) for diploid alleles that can occur by: (1) IBD, (2) uniparental disomy,[33] or (3) a large deletion CNV.

Sanger Sequencing

To validate exome-identified candidate variants by an orthogonal, experimental DNA-sequencing method and segregate these variants in the families, we amplified target exons from genomic DNA by using conventional PCR (HotStar TaqDNA polymerase, QIAGEN) and high-GC-content long-range PCR (TaKaRa LA Taq, Clontech), and we analyzed PCR amplification products by Sanger sequencing (DNA Sequencing Core Facility at Baylor College of Medicine). If the exome-identified variant was not confirmed by Sanger sequencing or if segregation analysis showed inconsistency with Mendelian expectations under the hypothesized genetic model, then the variant was considered to be unlikely to contribute to the arthrogryposis trait.

Chromosomal Microarray Analysis for Genome-Wide CNV Detection

For individuals in whom we detected a CNV (individual BAB7128) through genome-wide sequencing data and bioinformatic CNV-detection tools,[34] or as part of the preliminary, low-resolution clinical genomics diagnostic studies such as karyotyping and low-resolution array comparative genomic hybridization (aCGH; individual BAB8145 and individual BAB9312), we performed Agilent's custom-designed whole-genome array (Baylor Genetics Laboratory, CMA version 11, design#079906) to confirm the CNV. All array procedures, including DNA fragmentation and labeling, array hybridization, washing, and scanning, were performed according to the manufacturer's instructions and previously described protocols[35] with minor modifications. Gender-matched female control (NA15510) DNA and male control (NA10851) DNA were obtained from Coriell cell repositories (Coriell Institute for Medical Research). Data processing and analyses were done with Agilent Feature Extraction Software (version 11.5, Agilent Technologies) and Agilent Genomic Workbench (edition 7.0.4.0, Agilent Technologies).

Droplet Digital PCR Mosaicism Analysis

Variants suspected to be in a mosaic state on the basis of exome read-depth ratios (vR/tR, variant reads/total reads) were further validated via an orthogonal experimental system on a BioRad QX200 ddPCR platform. Custom-designed fluorescent TaqMan probes targeting the mutant variant (FAM fluorescence) and the reference (HEX fluorescence) were multiplexed with common forward and reverse primers and run under standard ddPCR conditions.[36] The fractional abundances for the amplified mutant and reference allele were calculated to determine the percent of the mosaicism.

Human and Fruit Fly Cross-Database Mining for Candidate Gene Analyses

We evaluated orthologs and paralogs in fruit flies and humans for identified candidate disease genes. In order to determine the human paralogs for fruit fly genes, we used DRSC Integrative Ortholog Prediction Tool (DIOPT).[37] We first forward checked the human gene in the fruit fly, and fly genes with the highest DIOPT scores were reverse checked to detect the number of human homologs. A DIOPT score of 3 is set as the threshold to determine the presence of paralogs or orthologs in the human or fly, respectively.

Results

Exome Sequencing and Family-Based Genomics in Arthrogryposis

We applied ES in a large cohort (Figure 1A, phase II) of 69 newly recruited families, a clinically heterogeneous group of individuals in whom the arthrogryposis phenotype is an apparent, isolated clinical feature (nonsyndromic arthrogryposis) or is part of the disease spectrum (syndromic arthrogryposis). Molecular findings from the analysis of phase I of this cohort had revealed a 58.3% (28 of 48

families studied) molecular diagnostic rate.[8] In phase II of this family-based genomics study, we analyzed 91 families, including 69 newly ascertained and recruited families, 20 families who remained "molecularly undiagnosed" from phase I, and two families identified through GeneMatcher (Figure 1A).

The results were divided into the five categories presented below: (1) known disease-associated genes that have an established association with the arthrogryposis phenotype; (2) "probably causative" arthrogryposis-associated genes: rare variant, likely to be damaging, pathogenic alleles present in at least two different families; (3) "possibly causative" arthrogryposis-associated genes: pathogenic variants discovered in only one family in this study; (4) oligogenic inheritance and blended phenotypes: multilocus pathogenic variation, i.e., variants present in at least two disease-associated genes, that explains the observed set of phenotypic features including arthrogryposis; (5) CNVs causing the arthrogryposis phenotype. The molecular findings of the individuals for the entire cohort are described in Tables 1, 2, S1, and S2, and Figures S1 and S2.

The overall molecular diagnostic rate in the present phase II cohort of 89 families with arthrogryposis is 65.2% (58/89); 43 of these 89 families have variants in previously described arthrogryposis-associated genes (six out of nine oligogenic families have both known and candidate genes). 18 out of 89 families, including both single locus and multilocus families, have variants in arthrogryposis-associated candidate genes. Three families were found to have CNVs that are thought to contribute to the arthrogryposis phenotype. Considering all families studied in both phase I[8] and phase II, we achieved a molecular diagnostic rate of 73.5% (86/117) when considering both known and potential disease genes, and 58.1% (68/117) of families had a molecular diagnosis involving a known disease gene.

Of note, the rate of consanguinity, as measured by AOH, was significantly higher in the molecularly diagnosed individuals compared to undiagnosed cohort individuals (60/86 = 69.8% in diagnosed cohort versus 5/31 = 16.1% in the undiagnosed cohort, $p < 0.0001$ Fisher's exact two-tailed test). However, we did not observe a significant difference in evidence for consanguinity in syndromic versus non-syndromic arthrogryposis in the diagnosed compared to undiagnosed individuals (30/86 = 34.9% in the diagnosed cohort versus 8/31 = 25.8% in the undiagnosed cohort, $p = 0.3824$ Fisher's exact two-tailed test). In the current study, we propose five probably causative and ten possibly causative arthrogryposis-associated genes and four candidate DD-and-ID-associated genes contributing to the disease phenotype (Figure 1B). Potential multilocus pathogenic variation, i.e., the oligogenic model, was observed in 11 families in this phase II cohort, specifically in 19.0% (11/58) of individuals with a diagnosis. The overall potential oligogenic inheritance rate including both phase I and phase II studies is 22.1% (19/86) of diagnosed individuals (Figure 1C).

Known Arthrogryposis-Associated Genes

A total of 43 families have a pathogenic variant in a gene associated with either nonsyndromic (isolated) or syndromic arthrogryposis (Tables 1, 2, and S1, and Figures S1 and S2). The most common identified molecular diagnoses and implicated genes included *CHRNG* (MIM: 100730), associated with Escobar syndrome and lethal multiple pterygium syndrome (EVMPS [MIM: 265000] and LMPS [MIM: 253290], respectively), in 12 of 116 Turkish families (10.3%, excluding the individual of Arabic origin in phase I), and *ECEL1* (MIM: 605896), associated with distal arthrogryposis type 5D (DA5D [MIM: 615065]) in six families. The calculated total AOH after we used BafCalculator on exome-generated variant data[31] was on average 218.66 Mb for these 18 families, whereas the average calculated total AOH size in the entire Turkish cohort (~700 exomes) is 91.38 Mb. Rare variants in *KLHL7* (MIM: 611119), previously associated with cold-induced sweating syndrome (CISS3 [MIM: 617055]), were identified in four unrelated families with syndromic primarily distal arthrogryposis. The syndromic features were characterized by variable involvement of the genitourinary system, DD and ID, and congenital heart disease, each in at least two families; these features represent a potential expansion of the known disease phenotypes associated with *KLHL7*. Additional molecular diagnoses reported in more than one family involved *MYH3* (MIM: 160720), associated with several forms of distal arthrogryposis (DA2A [MIM: 193700], DA2B [MIM: 601680], and DA8 [MIM: 178110]) in two families, and *SPEG* (MIM: 615950), linked to centronuclear myopathy 5 (CNM5 [MIM: 615959]). In total, rare variants in 45 different known genes were found within 43 families (including oligogenic families), and these findings reveal the extensive genetic heterogeneity in the arthrogryposis cohort. Additionally, we identified a second family with variants in *MYBPC2* (MIM: 160793), first proposed as a candidate arthrogryposis-associated gene in the phase I study.

Probably Causative Arthrogryposis-Associated Genes

We found evidence for five candidate genes, *RYR3* (MIM: 180903), *MYOM2* (MIM: 603509), *ERGIC1* (MIM: 617946), *SPTBN4* (MIM: 606214), and *ABCA7* (MIM: 605414), in which predicted deleterious variants are likely to be contributing to and probably causing the arthrogryposis phenotype; the variants likely to be pathogenic are present in at least two families, and additional families were identified either within our cohort, through GeneMatcher, or in recent publications (molecular findings in Tables 1, 2, and S1, and Figures S1 and S2; clinical findings in the Supplemental Text). For each of these genes, additional data, such as minor allele frequencies, evolutionary conservation, and CADD-phred scores of identified variants, that support their candidacy as arthrogryposis genes are provided (Tables 1, 2, and S1). These genes were not previously linked to any human disease in OMIM, or there has been only

Table 1. Molecular Summary of the Known, Probably, and Possibly Causative Arthrogryposis Genes in the Cohort

Gene	Proband	Nucleotide (Protein)	Zygosity	AOH Block Around the Gene (Mb)	Total AOH (Mb)
Known Causative Genes					
CHRNG	BAB8511	c.753_754del (p.Val253Alafs*44)	Hmz	20.8	162.1
	BAB8571	c.256C>T (p.Arg86Cys)	Hmz	25.8	251.1
	BAB8603	c.256C>T (p.Arg86Cys)	Hmz	6.7	154.5
	BAB8685	c.753_754del (p.Val253Alafs*44)	Hmz	19.0	248.8
	BAB9851	c.753_754del (p.Val253Alafs*44)	Hmz	22.3	123.3
	BAB9942	c.256C>T (p.Arg86Cys)	Hmz	3.5	557.7
ECEL1	BAB8223	c.1630C>T (p.Arg544Cys)	Hmz	3.3	199.2
	BAB9537	c.1581+1G>A	Hmz	14.2	164.4
	BAB10711	c.1916C>T (p.Ser639Phe)	Hmz	14.7	238
NEB	BAB8518	c.24988C>T (p.Arg8330*)	Hmz	73.4	151.2
COL12A1	BAB8843	c.1488dup (p.Phe497Ilefs*5)	Hmz	20.8	297.9
KLHL7	BAB8095	c.1051C>T (p.Arg351*)	Hmz	14.1	36.2
	BAB8098			21.7	96.5
	BAB8652	c.1022del (p.Leu341Trpfs*9)	Hmz	15.5	248.5
	BAB10699	c.565C>T (p.Arg189*)	Hmz	26.0	354.3
	BAB10705			22.9	238.2
MYBPC1	BAB8515	c.32A>G (p.Glu11Gly)	Hmz	25.8	351.9
MYBPC2	BAB9540	c.920T>C (p.Val307Ala)	Comp Htz	–	156.1
		c.3194C>T (p.Ala1065Val)			
MFN2	BAB3941	c.526G>A (p.Gly176Ser)	Hmz	0.8	99.6
SYNE1	BAB7084	c.2839G>A (p.Glu947Lys)	Comp Htz	–	17.7
		c.21164A>G (p.Lys7055Arg)			
PLEC	BAB7079	c.6523A>G (p.Lys2175Glu)	Comp Htz	–	8.2
		c.8813C>T (p.Thr2938Met)			
POR	BAB8694	c.859G>C (p.Ala287Pro)	Hmz	13.5	102.8
HSD17B4	BAB8832	c.1417C>T (p.Arg473Trp)	Hmz	49.0	202.9
	BAB8835			60.7	165.3
POMGNT1	BAB8986	c.461C>A (p.Pro154His)	Hmz / Hmz	29.3	168.4
		c.550C>T (p.His184Tyr)			
FKBP10	BAB9244	c.890_897dup (p.Gly300*)	Hmz	4.3	154.5
TGFB3	BAB9703	c.171del (p.Glu58Serfs*4)	Hmz	48.5	183.4
	BAB9704			30.1	480.7
TTN	BAB7779	c.2370+2T>C	Comp Htz	–	34.2
		c.67279C>T (p.Arg22427*)			
IGF1	BAB9740	c.156dup (p.Leu53Alafs*5)	Hmz	15.7	289.3
	BAB9741			6.6	208.3
TOR1A	BAB10702	c.506T>C (p.Phe169Ser)	Hmz	11.8	196.4
MYH3	BAB3964	c.2015G>A (p.Arg672His)	Htz	–	30.4
	BAB9848			–	26.1

(*Continued on next page*)

Table 1. ***Continued***

Gene	Proband	Nucleotide (Protein)	Zygosity	AOH Block Around the Gene (Mb)	Total AOH (Mb)
TNNT3	BAB3928	c.163C>T (p.Arg55Cys)	Htz	–	10.4
SYT2	BAB7308	c.1081G>C (p.Asp361His)	Htz	–	65.5
PIEZO2	BAB8789	c.8181_8183del (p.Glu2727del)	Htz	–	208.2
TRPV4	BAB8991	c.806G>A (p.Arg269His)	Htz	–	39.5
PQBP1	BAB8090	c.463C>T (p.Arg155*)	Hemi	–	24.2
Probably Causative Genes					
RYR3	BAB7845	c.2486G>A (p.Arg829His)	Hmz	1.8	247.5
	PAED187	c.2000A>G (p.Asp667Gly)	Comp Htz	–	5.5
		c.11164+1G>A			
	BAB8988	c.8939G>T (p.Arg2980Leu)	Hmz	12.0	149.6
MYOM2	BAB8905	c.621C>G (p.Ser207Arg)	Hmz	7.2	312.9
	IN076	c.2797C>T (p.Gln933*)	Hmz	7.2	369.1
ABCA7	BAB6807	c.5092C>T (p.Arg1698Trp)	Hmz	3.8	153.9
	BAB6808			3.0	180.2
	BAB10708	c.3076C>T (p.Arg1026Cys)	Comp Htz	–	233.8
		c.4045C>T (p.Arg1349Trp)			
ERGIC1	BAB8802	c.782G>A (p.Gly261Asp)	Hmz	30.8	274.6
SPTBN4	BAB8691	c.6433G>A (p.Ala2145Thr)	Hmz	3.4	183.9
Possibly Causative Genes					
MID1IP1	BAB8397	c.297C>G (p.Asn99Lys)	Hemi	–	374.7
DRG1	BAB8807	c.118C>T (p.Arg40*)	Hmz	7.6	251.6
TANC1		c.2830C>T (p.His944Tyr)	Hmz	10.3	
MYOM3	BAB8532	c.3534+56C>T	Comp Htz	–	107.2
		c.1684G>A (p.Val562Ile)			
TNRC6C	BAB8688	c.1022G>A (p.Gly341Glu)	Hmz	7.0	132.0
FLII	BAB7710	c.2590C>T (p.Arg864Trp)	Hmz	2.2	257.4
TAF9B	BAB8400	c.133C>A (p.Arg45Ser)	Hemi	–	110.6
MED27	BAB8606	c.770C>T (p.Pro257Leu)	Hmz	11.8	195.2
	BAB8609			2.0	233.7
CACUL1	BAB9729	c.910_911del (p.Leu304Ilefs*3)	Hmz	10.0	158.9
FGFRL1	BAB3944	c.124C>T (p.Arg42Trp)	Hmz	3.4	290.2
TMEM214	BAB5192	c.764G>A (p.Arg255Gln)	Hmz	15.9	220.3
NR2C1	BAB8086	c.544+1G>C	Hmz	4.3	231.7
	BAB8087			6.7	126.3
PRDM2	BAB9309	c.4283_4295del (p.Leu1428Glnfs*15)	Htz	–	284.5
FAT1	BAB8356	c.6026A>G (p.Asn2009Ser)	Hmz	2.0	142.9

Abbreviations are as follows: Mb = megabase, AOH = absence of heterozygosity, Hmz = homozygous, Hemi = hemizygous, Htz = heterozygous, and Comp Htz = compound heterozygous.

one reported individual, family, or variant; thus, we consider the variants within these genes to be probably causative for the arthrogryposis phenotype.

RYR3

RYR3 bi-allelic variants were found in three unrelated individuals (Table 1 and Figure 2): one was found as part of a

Table 2. Molecular Summary of the Multilocus Pathogenic Variation Cohort

Family ID (HOU#)	Proband ID (BAB#)	Gene	Nucleotide (Protein)	Zygosity	AOH Block Around the Gene (Mb)	Total AOH (Mb)
HOU2523	BAB6807	*COL6A3*	c.619C>T (p.Gln207*)	Hmz	7.8	153.9
		ABCA7	c.5092C>T (p.Arg1698Trp)	Hmz	3.8	
	BAB6808	*ABCA7*	c.5092C>T (p.Arg1698Trp)	Hmz	3.0	180.2
		ADNP	c.775A>C (p.Asn259His)	Hmz	–	
HOU2790	BAB7710	*ECEL1*	c.505_529del (p.Gly169Serfs*26)	Hmz	20.1	257.4
		FLII	c.2590C>T (p.Arg864Trp)	Hmz	2.2	
HOU2817	BAB7845	*RYR3*	c.2486G>A (p.Arg829His)	Hmz	1.8	247.5
		MYO18B	c.2879C>T (p.Ala960Val)	Comp Htz	–	
			c.3397C>T (p.Arg1133Trp)		–	
HOU3050	BAB8397	*NEB*	c.19101+5G>A	Hmz	–	374.7
		MID1IP1	c.297C>G (p.Asn99Lys)	Hemi	–	
HOU3051	BAB8400	*GBE1*	c.1864_1866del (p.Leu622del)	Hmz	37.9	110.6
		AP4M1	c.136C>G (p.Pro46Ala)	Hmz	14.2	
		TAF9B	c.133C>A (p.Arg45Ser)	Hemi	–	
HOU3112	BAB8532	*SPEG*	c.6971T>A (p.Ile2324Asn)	Hmz	22.6	107.2
		MYOM3	c.1684G>A (p.Val562Ile)	Comp Htz	–	
			c.3534+56C>T			
		CIT	c.2651A>C:p.Gln884Pro	Htz	–	
HOU3125	BAB8600	*FBN2*	c.4094G>C (p.Cys1365Ser)	Htz	–	–
	BAB8601	*FBN2*			–	31.9
		COL6A3	c.367G>A (p.Val123Met)	Hmz	1.5	
HOU3127	BAB8606	*COG6*	c.726del (p.Cys242Trpfs*7)	Hmz	16.9	195.2
		MED27	c.770C>T (p.Pro257Leu)	Hmz	11.8	
	BAB8609	*MED27*	c.770C>T (p.Pro257Leu)	Hmz	2.0	233.7
HOU3149	BAB8688	*KLHL7*	c.1258C>T (p.Arg420Cys)	Hmz	17.9	132.0
		HOXA11	c.304G>A (p.Val102Met)	Hmz	17.9	
		TNRC6C	c.1022G>A (p.Gly341Glu)	Hmz	7.0	
HOU3180	BAB8807	*DRG1*	c.118C>T (p.Arg40*)	Hmz	6.7	251.6
		TANC1	c.2830C>T (p.His944Tyr)	Hmz	10.3	
		BRWD3	c.592-3T>C	Hemi	–	
HOU3943	BAB10708	*SPEG*	c.9575C>A (p.Thr3192Asn)	Htz	–	233.8
		TPM2	c.620_631dup (p.Gln210_Ala211insValGluAlaGln)	Htz	–	
		ABCA7	c.3076C>T (p.Arg1026Cys)	Comp Htz	–	
			c.4045C>T (p.Arg1349Trp)		–	

Abbreviations are as follows: Mb = megabase, AOH = absence of heterozygosity, Hmz = homozygous, Hemi = hemizygous, Htz = heterozygous, and Comp Htz = compound heterozygous.

potential multilocus mutational burden disease model (*RYR3* + *MYO18B* [MIM: 607295]) (individual BAB7845), one was identified through GeneMatcher (individual PAED187), and one was found by assuming a single-gene-single-disease model (individual BAB8988). The first individual, BAB7845, is a 6-month-old female who was born to a first degree cousin marriage with 247.5 Mb of total AOH. The proband exome revealed a compound-heterozygous variant in a known gene, *MYO18B* (GenBank: NM_032608; c.[2879C>T]; [3397C>T]: p.[Ala960Val];

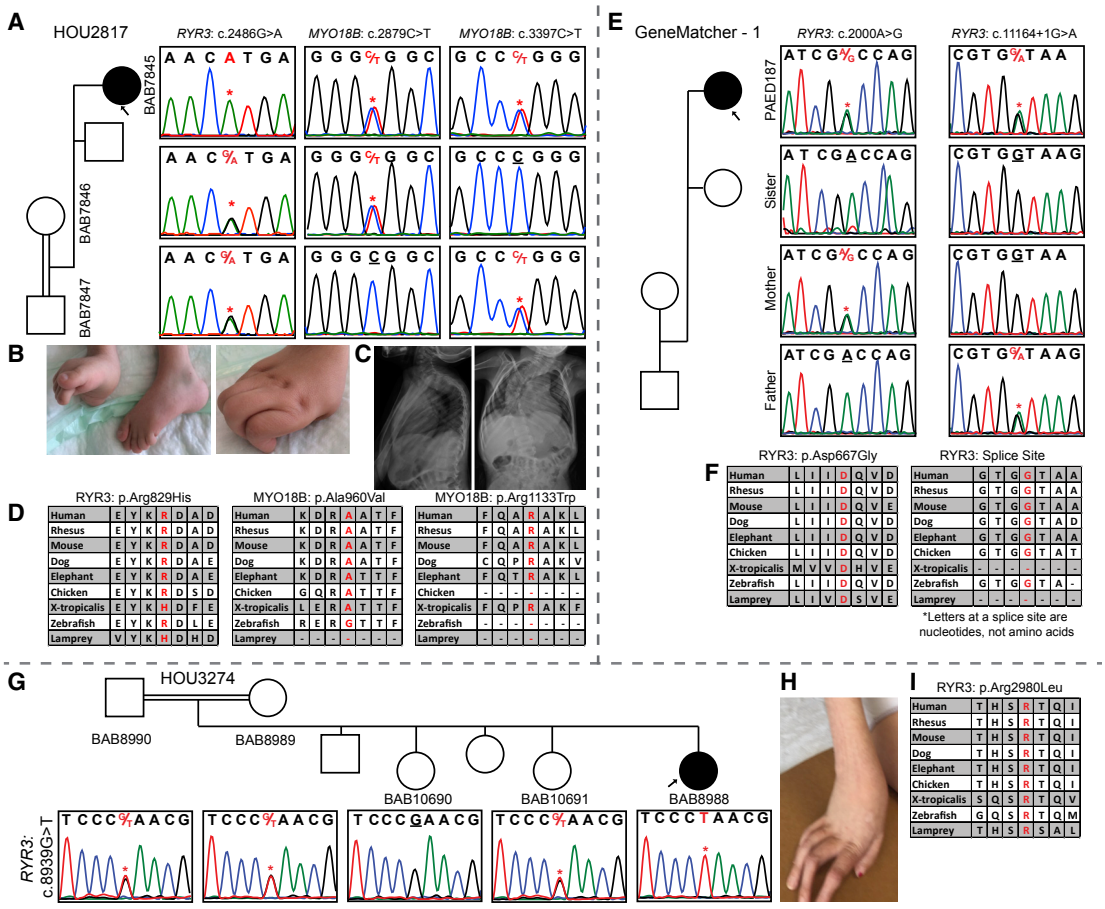

Figure 2. Segregation Results, Images, and Variant Distributions of the Individuals with *RYR3* Mutation
(A) Sanger studies showing compound-heterozygous variants in *MYO18B* and a homozygous variant in *RYR3* in the proband of family HOU2817.
(B) Pictures of the proband's contractures in fingers and toes.
(C) Anterior-posterior and lateral views of spinal X-ray showing the kyphoscoliosis.
(D) Conservation of the three variants through species. Variants of interest are written with a red font.
(E) Segregation studies for both the c.2000A>G and c.11164+1G>A variants in GeneMatcher – 1.
(F) Highly conserved asparagine (D) amino acid and splice site through species.
(G) A pedigree and Sanger segregation of family HOU3274 that had a single affected female individual (BAB8988) and two unaffected siblings available for study. Both parents and one unaffected sibling are heterozygous, the second unaffected sibling is wild type, and our proband is homozygous for the c.8939G>T variant.
(H) A colored picture of the hand showing the contractures in the fingers of individual BAB8988.
(I) The arginine (R) amino acid residue is highly conserved among species and specified in red font.

[Arg1133Trp]), and a homozygous variant in *RYR3* (GenBank: NM_001243996; c.2486G>A [p.Arg829His]) (Figures 2A–2D). The c.2879C>T *MYO18B* variant and the *RYR3* variant were each reported as homozygous in one individual in gnomAD. On the basis of the amino acid conservation and "likely damaging prediction scores" (Table S1) of the variants identified herein, we propose that all three variants are hypomorphic alleles, and each contributes to the arthrogryposis phenotype in this individual. Variants in *MYO18B* were recently shown to cause a neuromuscular disease spectrum ranging from nemaline myopathy with cardiomyopathy to Klippel-Feil anomaly with myopathy (KFS4 [MIM: 616549]),[38,39] and here we report the fourth family with *MYO18B* variants. Individual PAED187 has compound heterozygosity for a missense variant (GenBank: NM_001036.3; c.2000A>G [p.Asp667Gly]) and a variant affecting the splice donor (c.11164+1G>A) in *RYR3* (Figures 2E and 2F). Individual BAB8988 was born to first degree cousin parents with 149.6 Mb of total AOH according to BafCalculator. Trio ES revealed a homozygous nonsynonymous change in *RYR3* (GenBank: NM_001243996; c.8939G>T [p.Arg2980Leu]) (Figures 2G–2I). Recently, compound-heterozygous alleles in *RYR3*, c.[6208A>G]; [8939G>T]: p.[Met2070Val]; [Arg2980Leu], were reported in a 22-year-old female with myopathic facies, proximal weakness in all four limbs, mild scapular winging, and type 1 muscle fiber atrophy and predominance in muscle biopsy.[40] The c.8939G>T variant in the reported individual is the same variant observed in individual BAB8988.

The ryanodine receptors are intracellular Ca^{2+} release channels that play a key role in cell signaling via Ca^{2+}.

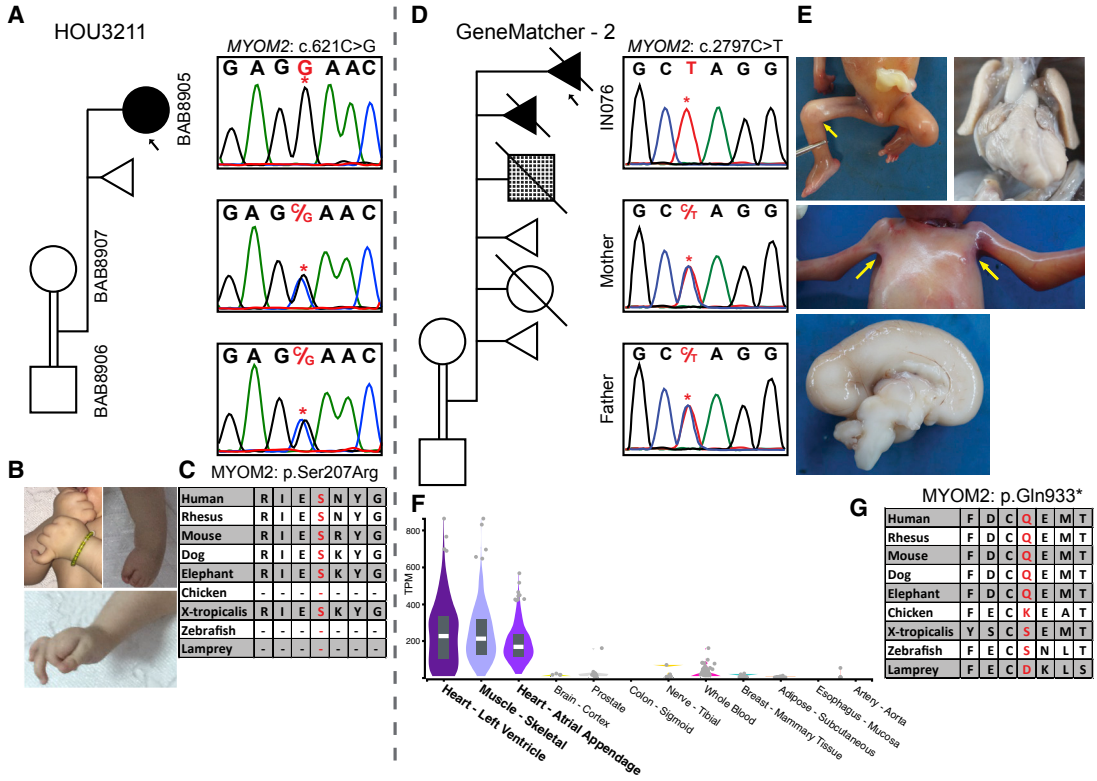

Figure 3. Clinical and Molecular Details of the *MYOM2* Individuals

(A) Pedigree and segregation analyses of the identified *MYOM2* variant (c.621C>G) in family HOU3211. The parents are shown as consanguineous because they are from the same small village and the proband demonstrates large AOH blocks on exome data. As expected with a recessive inheritance pattern, the parents are heterozygous and the proband (individual BAB8905) is homozygous for the c.621C>G variant.

(B) Proband's photos showing the contractures in the hands and feet.

(C) High conservation of the Ser207 amino acid in other species. The serine (S) amino acid is written with a red font color.

(D) A pedigree of the family (GeneMatcher – 2) showing a complicated medical history including affected and unaffected deceased siblings along with medically terminated or spontaneously aborted individuals in the GeneMatcher family. The fourth pregnancy is shown with a checkered box to indicate a different phenotype than neuromuscular disease (i.e., he was found to have cardiac and gastrointestinal anomalies along with intrauterine growth restriction). Sanger PCR from available individuals shows that the affected fetus is homozygous and the parents are heterozygous for the c.2797C>T variant.

(E) Pictures of the fetus showing pterygia of axillae and popliteal joints and a midsagittal cut of fetal brain showing partial agenesis of the corpus callosum and bilateral hypoplastic lungs.

(F) A genotype-tissue expression (GTEx) panel showing specific expression of *MYOM2* in skeletal and heart muscles.

(G) Amino acid conservation around Gln933 among other species. The Gln (Q) amino acid is written in red font.

RYR1 (MIM: 180901) plays a role in the initial voltage-dependent Ca^{2+} release, and RYR3 functions during the prolonged Ca^{2+} release.[41,42] Further evidence that the pathogenicity of the variants in *RYR3* probably contribute to the arthrogryposis phenotype comes from bioinformatics studies; Abath Neto et al. performed a computational data-mining study based on gene ontology (GO) terms, human phenotype ontology (HPO) terms, pathways, complexes, and protein motifs, and they found that *RYR3* is highly ranked as one of the congenital myopathy genes.[43] Mutations in *RYR1*, a paralog of *RYR3*, were shown to cause several neuromuscular disorders including central core disease (CCD [MIM: 117000]), myopathies (MIM: 255320 and 117000), and the complex trait of susceptibility to malignant hyperthermia (MHS1 [MIM: 145600]), a sometimes lethal disease induced by exposure to certain anesthetics during surgical interventions; deleterious variants in *RYR2* (MIM: 180902) were known to cause cardiac rhythm disorders (ARVD2 [MIM: 600996] and CPVT1 [MIM: 604772]), whereas no disease has been linked to *RYR3*. Taken together, we propose pathogenic variants in *RYR3* are causing neuromuscular disease on the basis of the presence of deleterious variants in three unrelated families and functional evidence for its involvement in neuromuscular disease.

MYOM2

Two unrelated individuals carry variants in *MYOM2* (Figure 3). Trio ES revealed a homozygous missense variant (GenBank: NM_003970; c.621C>G [p.Ser207Arg]) in Myomesin-2 (*MYOM2*) in individual BAB8905 (Figures 3A–C). The second individual, a fetus terminated at 20 weeks of gestation (found through GeneMatcher) (individual IN076), was found to have a homozygous nonsense variant and presumed null allele (GenBank: NM_003970; c.2797C>T [p.Gln933*]) in *MYOM2* (Figures 3D–G). Because

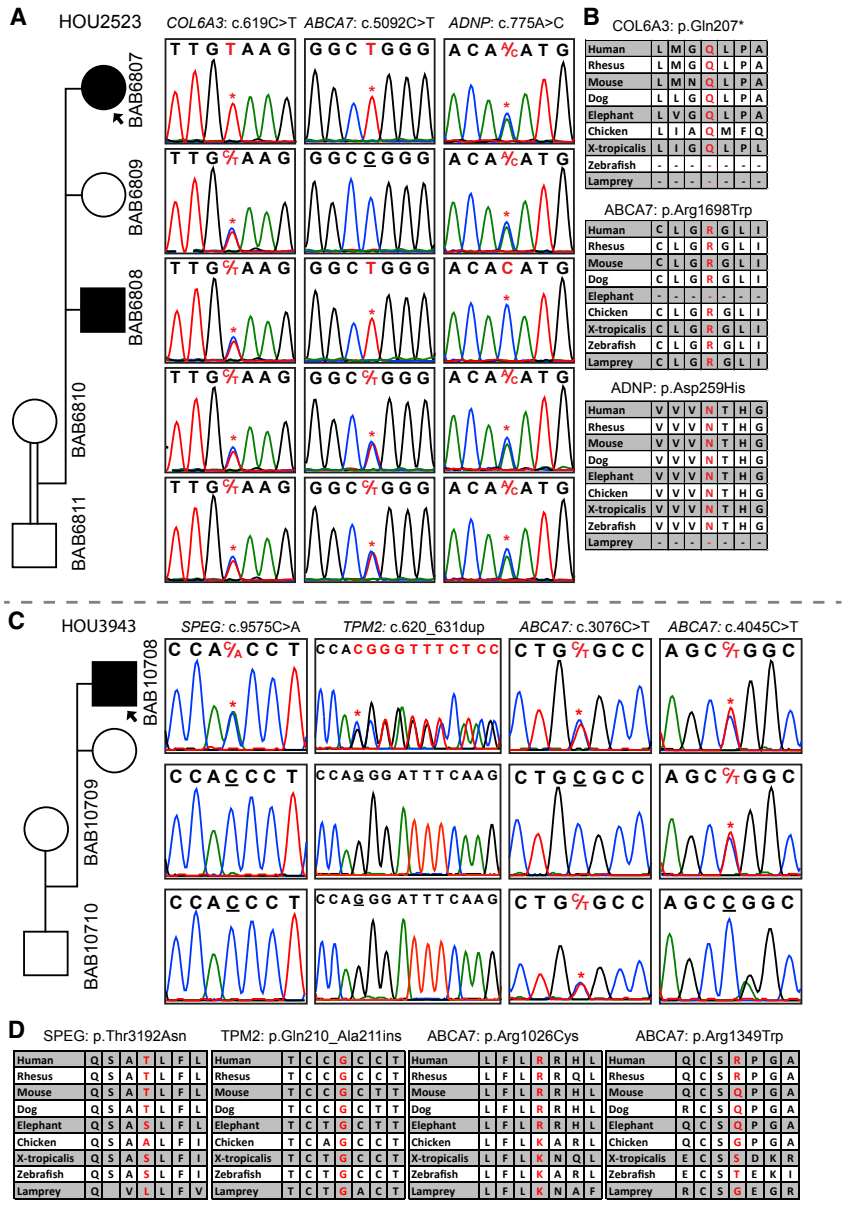

Figure 4. Families with *ABCA7* Variants
(A) A pedigree suggesting an autosomal-recessive inheritance pattern for *ABCA7*, *COL6A3*, and *ADNP* in family HOU2523; the affected individuals are homozygous, whereas unaffected individuals are heterozygous. Individual BAB6807 has a homozygous stop-gain mutation in *COL6A3* in addition to a homozygous *ABCA7* variant shared with individual BAB6808. The *ADNP* variant is homozygous in individual BAB6808, who has a DD and ID phenotype.
(B) Conservation profiles of all three genes.
(C) A pedigree of family HOU3943 with segregation studies showing bi-allelic variants in *ABCA7* and *de novo* heterozygous variants in *SPEG* and *TPM2*.
(D) The amino acid alignment of the detected variants across different species.

MYOM2 is specifically expressed in the heart and skeletal muscle, the cardiac and arthrogryposis findings can be potentially explained by loss of function (LoF) mutation of *MYOM2*. Further evidence for probable pathogenicity comes from functional studies that showed that MYOM2 interacts directly with dysferlin, which plays an essential role in sarcolemma repair; abnormalities of dysferlin cause a wide variety of myopathies called dysferlinopathies.[44]

ABCA7

Bi-allelic *ABCA7* variants were found in two unrelated families (Figure 4). In the first family, there were two affected siblings, individuals BAB6807 and BAB6808 (Figures 4A and4B). The younger female sibling was more severely affected with arthrogryposis, whereas the older male sibling, individual BAB6808, was observed to have DD and ID in addition to a neuromuscular phenotype. ES was performed on both affected siblings. Individual BAB6807 was found to have a novel homozygous stop-gain mutation (GenBank: NM_057166; c.619C>T [p.Gln207*]) in the known *COL6A3* gene (MIM: 120250), but the affected brother and healthy parents were heterozygous for this variant. Given the relative phenotypic similarity between the two affected siblings (the female is more severely affected, and the brother had additional DD and ID phenotype), we searched for variants shared by the two affected siblings and found a homozygous missense change (GenBank: NM_019112; c.5092C>T [p.Arg1698Trp]) in ATP-binding cassette, subfamily A, member 7 (*ABCA7*). Individual BAB6808, who has an additional DD and ID phenotype, was found to carry a deleterious homozygous variant (GenBank: NM_015339; c.775A>C [p.Asn259His]) in *ADNP* (MIM: 611386), in which variants are known to cause DD and ID (HVDAS [MIM: 615873]).[45] The homozygous *COL6A3* variant in individual BAB6807 probably explains the more severe phenotype in this individual. In the second family, individual BAB10708 is found to have variants in three different genes: (1) compound-heterozygous deleterious variants in *ABCA7* (GenBank: NM_019112; c.[3076C>T]; [4045C>T]: p.[Arg1026Cys]; [Arg1349Trp]), (2) a *de novo* heterozygous variant in *SPEG* (MIM: 615950; GenBank: NM_005876; c.9575C>A [p.Thr3192Asn]), in which bi-allelic variants are known to cause centronuclear myopathy 5 (CNM5 [MIM: 615959]), and (3) a *de novo*, heterozygous, non-frameshift insertion in *TPM2* (MIM: 190990; GenBank: NM_003289; c.620_631dup [p.Gln210_Ala211insValGluAlaGln]), in which monoallelic variants are known to cause a broad spectrum of neuromuscular disorders including distal arthrogryposis

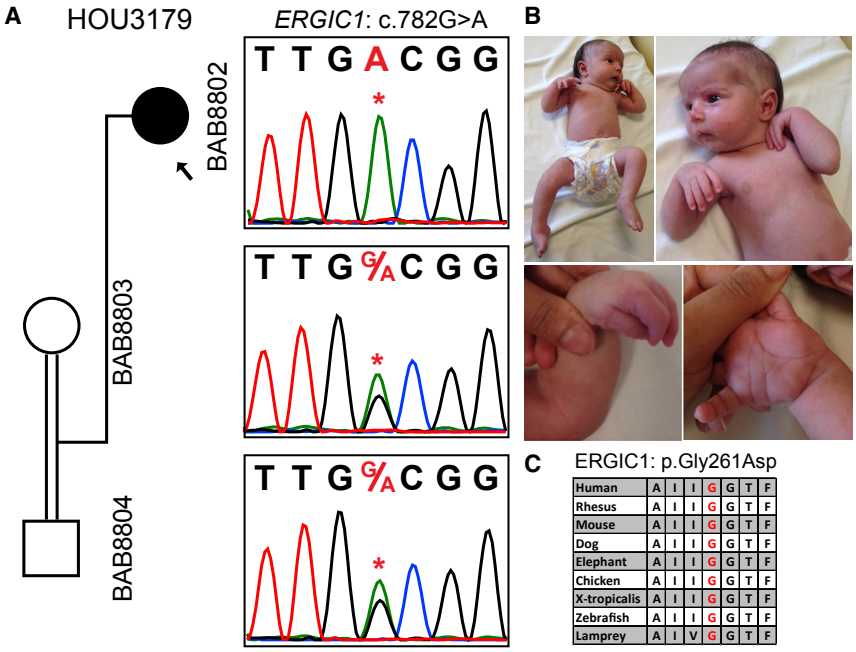

Figure 5. Segregation, Pictures, and Protein Conservation for a Homozygous *ERGIC1* Variant in Individual BAB8802

(A) Segregation analyses of the exome-detected variant; the proband was homozygous and the parents were heterozygous carriers, as expected in recessive disease traits.

(B) Proband photographs showing restrictions in the wrists and fingers and the *pes equinovarus* deformity in the feet.

(C) A peptide alignment showing the conservation of the affected amino acid across species.

multiplex congenita types 1 and 2B (DA1A [MIM: 108120] and DA2B [601680]) (Figures 4C and 4D). Heterozygous variants in *ABCA7* have been linked to Alzheimer susceptibility (AD9 [MIM: 608907]); however, bi-allelic variants associated with recessive trait variants have not been reported in any diseases previously. ATP-binding cassette (ABC) proteins transport various molecules across extra- and intra-cellular membranes. Heterozygous variants in *ABCA1* (MIM: 600046) are associated with type 2 HDL deficiency and protection against coronary artery disease in familial hypercholesterolemia (MIM: 604091 and 143890, respectively), and homozygous variants in *ABCA1* are known to cause Tangier disease (TGD [MIM: 205400]), which has clinical features of distal muscle atrophy and peripheral neuropathy. As per the STRING database, there is distant interaction between *ABCA1* and *ABCA7*.

ERGIC1

Trio ES of individual BAB8802 showed a homozygous change (GenBank: NM_001031711; c.782G>A [p.Gly261Asp]) in *ERGIC1* (Figure 5). This gene was reported in a large family affected with arthrogryposis multiplex congenita; in this family, 40 affected individuals were found to have c.293T>A (p.Val98Glu), cosegregating with the AR disease trait.[46] However, to date, no additional families or variants in *ERGIC1* have been associated with arthrogryposis. ERGIC (ER-Golgi intermediate compartment) family proteins are transmembrane proteins that are localized to the ER-Golgi intermediate compartment, but the function of ERGIC1 remains elusive.[47] The observation of a second family with rare variation in *ERGIC1* in association with arthrogryposis strengthens its relevance to the arthrogryposis phenotype.

SPTBN4

Trio ES revealed a homozygous GenBank: NM_020971; c.6433G>A (p.Ala2145Thr) variant in *SPTBN4* in individual BAB8691, who presented with distal contractures, hearing loss, and DD and ID (Figure 6). Recently, Knierim et al. reported a homozygous nonsense variant GenBank: NP_066022.2; p.Gln533* in a male with myopathy, distal arthrogryposis, scoliosis, hearing loss, severe DD and ID, increased cerebrospinal fluid (CSF) spaces on brain MRI, and peripheral neuropathy.[48] An immunoblot and immunostaining showed the absence of SPTBN4, and a knockout mouse model showed findings, including muscle weakness, decreased locomotion, quivering, ataxia, and hearing loss, that are similar to those in humans. Between these two individuals there is significant phenotypic overlap, including severe DD and ID, grossly normal brain MRI, hearing loss, distal contractures, and failure to thrive. Another homozygous variant (GenBank: NM_020971.2; c.3394del [p.His1132Thrfs*39]) of *SPTBN4* was reported by Anazi et al. in an individual who had no reported arthrogryposis but did have clinical features of global developmental delay, hypotonia, dysphasia, recurrent respiratory infections, blue sclerae, hyporeflexia, and failure to thrive.[49] Although the authors did not report any electromyography or nerve conduction studies, the clinical observation of hyporeflexia and hypotonia might be features of peripheral neuropathy. *SPTBN4* encodes a nonerythrocytic member of the beta-spectrin protein family that is mainly expressed in the brain, peripheral nervous system, pancreas, and skeletal muscle. Mutation of different domains might explain why each person presented with more central nervous system than neuromuscular features. Our individual has both neuromuscular and central nervous system findings and is the second individual now demonstrated to have arthrogryposis in association with a rare variant in *SPTBN4*; this supports that *SPTBN4* is associated with both DD and ID and with the arthrogryposis phenotype.

Possibly Causative Arthrogryposis-Associated Genes

We identified ten candidate arthrogryposis-associated genes (*CACUL1*, *DRG1* [MIM: 603952], *FAT1* [MIM: 600976], *FGFRL1* [MIM: 605830], *FLII* [MIM: 600362], *MID1IP1*

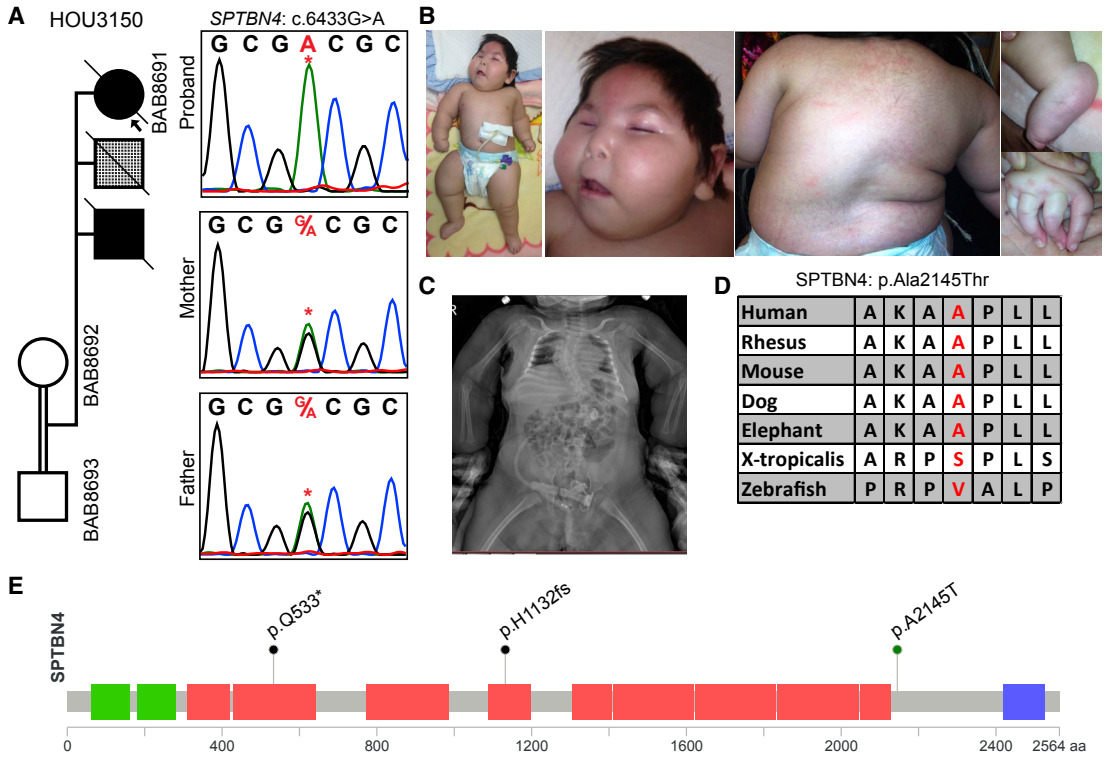

Figure 6. Clinical and Molecular Studies for a Homozygous *SPTBN4* Variant in Individual BAB8691
(A) Segregation studies showing heterozygosity for the parents and homozygosity for the index for variant c.6433G>A. The second child, who died of an unknown lung malformation, is shown with a checkered box.
(B) Pictures of the proband showing a myopathic face, scoliosis, contractures in the fingers, and *pes equinovarus* deformity in the feet.
(C) An anterior-posterior view of a spine X-ray showing severe thoracic scoliosis.
(D) High conservation of the mutated amino acid residue across species (red font).
(E) Protein domains of SPTBN4, with the variant identified in the present cohort (p.Ala2145Thr) and variants reported in two individuals in the literature (p.Gln533* and p.His1132fs).

[MIM: 300961], *MYOM3* [MIM: 616832], *NR2C1* [MIM: 601529], *PRDM2* [MIM: 601196], and *TMEM214* [MIM: 615301]) and four candidate DD-and-ID-associated genes (*MED27* [MIM: 605044], *TAF9B* [MIM: 300754], *TANC1* [MIM: 611397], and *TNRC6C* [MIM: 610741]) (Tables 1, 2, and S1, Figures S1–S4, and the Supplemental Text). Rare variants in each gene were identified in a single family, leading to their classification as candidate disease genes for which additional evidence is required before they are established as disease-associated genes. Evidence supporting plausible pathogenicity of these variant alleles includes amino acid conservation among other species, the predicted probably damaging effect of the variant made on the basis of bioinformatics tools, and interactome studies. Only two of these genes are highlighted here, and clinical and molecular results of all candidate genes are detailed in the oligogenic inheritance and blended phenotype section in Tables 1, 2, and S1, and the Supplemental Text.

Trio ES in individual BAB9729 revealed a homozygous 2 bp deletion (GenBank: NM_153810; c.910_911del [p.Leu304Ilefs*3]) in *CACUL1*, encoding a cell-cycle-associated protein capable of promoting cell proliferation through the activation of CDK2 at the G1/S phase transition (Figure S5). Interacting genes, *NEDD8* (MIM: 603171) and *FBXW7* (MIM: 606278), have a role in muscle function. Lange et al. showed that obscurin, a binding partner of titin, contains a non-modular C terminus that interacts with muscle specific isoforms of Ankyrin-1 (small Ankyrin-1.5; sAnk1.5).[50] sAnk1.5 localization and levels of sAnk1.5 expression are downregulated in obscurin knockout tissues, probably through ubiquitylation and/or neddylation of sAnk1.5.[50] Another interacting gene, *Fbxw7b*, negatively regulates differentiation, proliferation, and migration of myoblasts and satellite cells on muscle fibers.[51] The same group additionally showed that overexpression of *Fbxw7b* induces the expression of myogenin and major atrogene markers (atrogin-1 and MuRF-1) and eventually reduces myoblast differentiation.[52]

Trio ES in individual BAB9309 revealed a *de novo* frameshift deletion (GenBank: NM_012231; c.4283_4295del [p.Leu1428Glnfs*15]) in PR domain-containing protein 2 (*PRDM2* [MIM: 601196]). The fraction of variant reads (12/150, 8.0%) suggested somatic mosaicism, an experimental conclusion that was supported by an independent orthogonal experimental approach that used ddPCR (Figure 7A). PRDM2 is a member of a nuclear histone and protein methyltransferase superfamily and plays a major role in the regulation of myogenesis.[53,54]

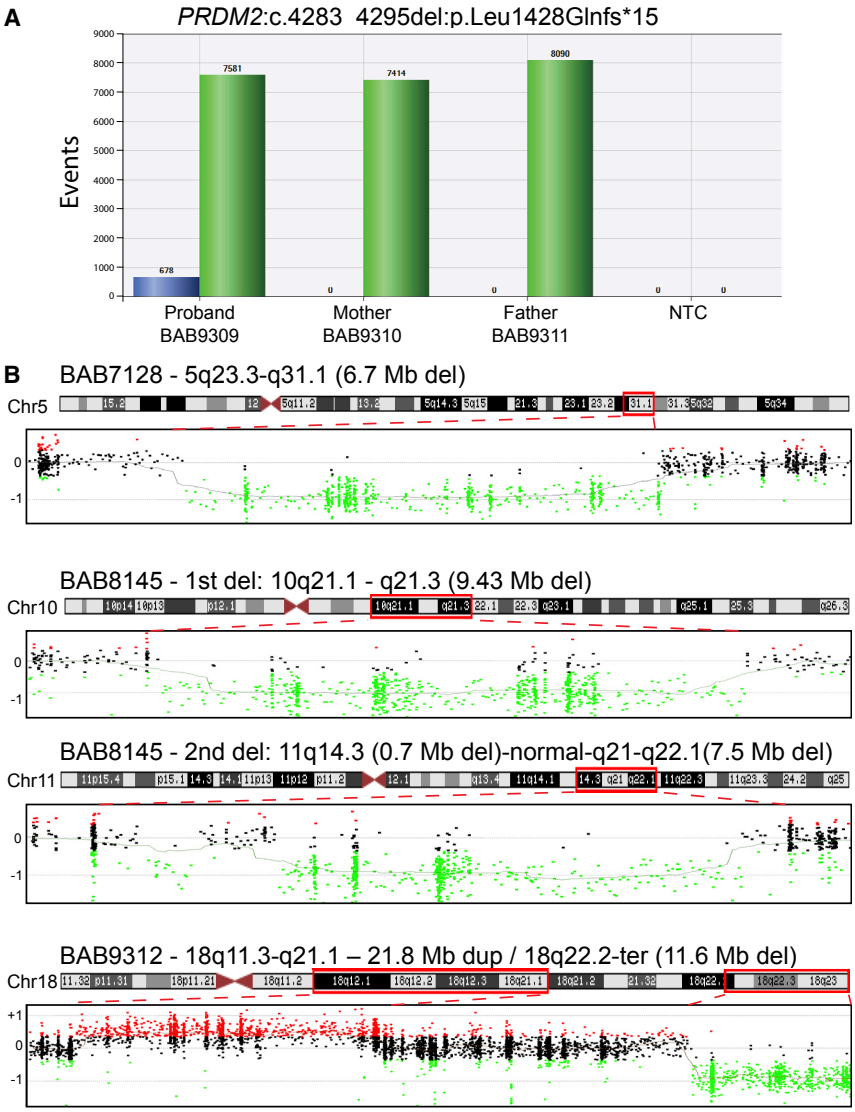

Figure 7. Molecular Studies in Individual BAB9309 and Copy Number Variant Families

(A) Droplet digital PCR (ddPCR) results for the family; the results show 8% mosaicism for the *PRDM2* variant in the proband, and this finding is consistent with the exome mosaicism rate (8%) and no deletion in the healthy parents.

(B) Results for aCGH analyses in three individuals are shown. Each dot indicates oligonucleotide probes: black dots represent a normal copy number, red dots represent a copy number gain, and green dots represent copy number losses as compared with a gender-matched control. The proband's designated ID (BAB#s), the chromosomal location, and the approximate sizes of the copy number variants (CNVs) are written above each chromosome ideogram, and the chromosome number is written on the left side of ideogram. Red dashed lines determine the chromosomal region investigated by aCGH. Abbreviations are as follows: Chr = chromosome, Del = deletion, Dup = duplication, Mb = megabase, NTC = no template control, and Ter = terminal.

CNVs in Arthrogryposis

In three individuals, we found CNVs that were probably contributing to the arthrogryposis phenotype (Figure 7B and Table S2). We searched the genomic intervals defined by these CNV regions in these three individuals for possible candidate dosage-sensitive genes; however, we could not readily identify any specific potentially dosage-sensitive genes. We also examined the DECIPHER database for additional individuals with CNVs involving the identified regions and found a few individuals with overlapping features in two of these three individuals (individuals BAB7128 and BAB9312). However, the overlapping region of CNV remained substantial and had multiple annotated genes within its boundaries, precluding identification of a single, potentially etiologic gene. Individual BAB7128 was a 20-month-old male with DD and ID, hearing loss, bilateral hip dislocation, and *pes equinovarus* (PEV) deformity. The CNV detection tool (XHMM) showed a 6.7 Mb *de novo* deletion that includes 54 genes in the deletion region on chromosome 5 (hg19.g.chr5: 129673070–136365890). A DECIPHER database search revealed four individuals (DECIPHER ID#s 785, 2224, 256078, and 260667) with scoliosis, distal arthrogryposis, camptodactyly, and/or PEV. The smallest overlapping region of ~2 Mb involving 11 genes (hg19.g.chr5: 129673070–131550089) was found in DECIPHER individual 785. This individual has camptodactyly and PEV, which partially explain our subject's clinical features. Individual BAB8145 was a 3.5-year-old female with DD and ID, contractures in fingers and toes, and PEV. She was found to have two *de novo* deletions: a 9.43Mb deletion in chromosome 10 (hg19.g.chr10: 58374373–67805420) involving 29 genes and a 0.7 Mb *de novo* deletion in a non-coding region on chromosome 11 (hg19.g.chr11: 90798107–91499657); this was followed by an ~1 Mb normal copy number and 7.58 Mb *de novo* deletion on chromosome 11 (hg19.g.chr11: 92950818–100534639) involving 39 genes in the region, and this was detected by karyotyping. Individual BAB9312 was a 7-year-old female who presented with DD and ID, hearing loss, and PEV. She was found to have a complex genomic rearrangement (CGR)[55] involving chromosome 18: a 21.8 Mb duplication (hg19.g.chr18: 21901302–43716565) and an 11.6 Mb deletion (hg19.g.chr18: 66350129–78002264) (Figure 7B). Interestingly, there were three DECIPHER individuals (# 251072, 269015, and 319532) with overlapping clinical features that included DD and ID, hearing loss, PEV, and additional clinical findings, but the overlapping region

was ~10 Mb in all three individuals (hg19.g.chr18: 67223975–77120273).

Families Potentially Affected by Multilocus Pathogenic Variation

Although many of the early cohort-based studies describing multiple molecular diagnoses involve known disease genes, there have been more recent reports of multiple molecular diagnoses for which one identified gene is a candidate gene proposed to explain the observed, expanded phenotype associated with a well-studied, known disease-associated gene.[10,14,31,56] Given the rarity of the conditions studied, it is unlikely that two or more unrelated families will share the same combination of multiple molecular diagnoses. However, apparent phenotypic expansion in the setting of a single molecular diagnosis can, in some individuals, suggest a second, or even third, molecular diagnosis explaining the observed, expanded phenotypic features.[31] Considering this possibility in the present cohort, we further explored 11 families for which there was evidence of multilocus pathogenic variation potentially contributing to the phenotype, i.e., mutational burden contributing to a blended phenotype (Tables 2 and S1, Figures S1 and S2, and the Supplemental Text).[10] Six out of 11 families have three genes with variants that are likely to be pathogenic and that we propose have an impact on the disease phenotype. We highlight one example from "known-known" and one example from "known-candidate" gene patterns, and the remainder of individuals with proposed multilocus pathogenic variation are detailed in Tables 2 and S1, Figure S2, and the Supplemental Text.

Trio ES in individual BAB8600 (index) and her more severely affected mother, individual BAB8601, revealed novel variants in two known genes, *FBN2* (MIM: 612570) and *COL6A3* (Figure S6). The variant in *FBN2* was a *de novo* missense change (GenBank: NM_001999; c.4094G>C [p.Cys1365Ser]) in the mother that was transmitted to the less severely affected child. The *COL6A3* variant (GenBank: NM_057167; c.367G>A [p.Val123Met]) was a homozygous missense change in the mother and heterozygous in the affected child and maternal grandparents. Mutations in *FBN2* are known to cause autosomal-dominant contractural arachnodactyly (DA9 [MIM: 121050]), whereas deleterious variants in *COL6A3* cause several neuromuscular phenotypes including dominantly and recessively inherited Bethlem myopathy 1 (BTHLM1 [MIM: 158810]). Additional features in the mother can potentially be parsimoniously explained by homozygosity for the identified variant in *COL6A3*.

Individual BAB8397 underwent trio ES, which showed a reported, homozygous splice-site variant (GenBank: NM_001271208; c.19101+5G>A) in *NEB* (MIM: 161650) and a hemizygous, i.e., X-linked in a male proband, nonsynonymous variant (GenBank: NM_001098791; c.297C>G [p.Asn99Lys]) in *MID1IP1* (Figure S7). The *NEB* variant identified in the proband was previously reported in a compound-heterozygous state with a nonsense variant (p.Tyr1858*) in an arthrogryposis-affected individual who died during the neonatal period.[57] The more severe phenotype in that individual could be explained by loss of function of the second allele. The second gene, *MID1IP1*, was not linked to any human disease previously. However, there are studies showing that *MID1IP1* probably plays a role in myogenesis.[58,59] Casey et al. showed that *Mid1ip1* expression is increased in the skeletal muscle of rats with peroxisome proliferator-activated receptors (PPAR)-induced myopathy.[58] Additionally, Bower et al. showed upregulation of *Mid1ip1* both with feeding and *in vitro* myogenesis in salmon fish.[59] The study further showed that *Mid1ip1* is highly expressed in fast and slow twitch muscle fibers compared to other tissues in the body. Although the function of *MID1IP1* is not fully delineated, taken together, these data provide evidence that the *MID1IP1* variant is likely to be contributing to the myopathy and contracture phenotype in our study individual.

The median total AOH size (individual locus AOH regions $\geq$3 Mb) calculated from exome data with BafCalculator in the probands with arthrogryposis and without any evidence for multilocus pathogenic variation (n = 97) is significantly higher (89.7 Mb) than the median total AOH size in the non-Turkish probands present in the Baylor-CMG database (n = 2,340) (23.5 Mb) (Mann-Whitney U test, p value = 7.35×10^{-17}). Intriguingly, the probands that were studied in this arthrogryposis cohort and had dual molecular diagnoses (n = 19) have a larger median total AOH size (159.3 Mb) than the median total AOH size of the probands without any dual molecular diagnosis (n = 97; 89.7 Mb) (Mann-Whitney U test, p value = 0.02).

Discussion

We investigated the underlying molecular etiology of a large cohort (totaling 117 families including the phase I cohort) of individuals with arthrogryposis, either as an isolated clinical entity or as part of a syndrome, by using genome-wide assays. The current phase II cohort consists of 91 families, including two families identified through GeneMatcher, and 20 families who remained undiagnosed during the phase I study: ten out of 20 families who remained undiagnosed during phase I underwent reanalysis, and we expanded the sequencing to additional family members (e.g., index ES to trio or quad ES) in the remaining ten families. Overall, the molecular diagnostic rate from the combined phase I and II families was 73.5% (86 out of 117) when including both known and candidate genes, and 58.1% (68 out of 117) when considering molecular diagnoses involving only known genes.

Some experimental analysis enhancements that were implemented in our phase II approach and that potentially contributed to the increase in the molecular diagnostic yield in the second cohort (65.1% in phase II versus 58.3% in phase I) are expanding to trio ES and

reanalyzing with additional bioinformatics tools the individuals from phase I who had unsolved molecular diagnoses. Multilocus pathogenic variation, consistent with a mutational burden or a potential oligogenic inheritance model, was observed in 19.0% (11/58) of the unrelated individuals with a molecular diagnosis in the present (phase II) cohort and 22.1% (19/86) of all 86 arthrogryposis-affected individuals with a molecular diagnosis reported here and in our previous [Phase I[8] + II] study. Although AOH is indeed predicted to increase the frequency of homozygous variants in this cohort, identified multiple molecular diagnoses involved at least one known disease-associated locus in each individual and included known pathogenic or premature truncating variants at six loci, and additional evidence for the pathogenicity of identified variants is provided (Table S1 and Figure S2). Parents who are carriers for multilocus variation are notably unaffected, and four families with intrafamilial phenotypic variation (families HOU2523, HOU2620, HOU2791, and HOU3125) provide an opportunity to further dissect the relationship between observed phenotypes and identified genotypes.

Our phase II study additionally contributed to the classification of five genes (*MYOM2*, *RYR3*, *ERGIC1*, *SPTBN4*, and *ABCA7*), in which variation is probably causative of the arthrogryposis phenotype because they have now been identified in more than one family with the same phenotype.

We previously studied human disease-associated genes by using the universality of biology and the bidirectional synergism between fly and human genetics; this showed that essential fly genes with multiple human paralogs are 8-fold more likely to be disease-causing genes.[60] We applied this approach to human paralogs for our proposed candidate genes in the arthrogryposis cohort and found that 14 of 19 have a fly ortholog, and 8 of 14 genes (including DD-and-ID-associated genes) have two or more human paralogs (Table S3).

Reanalysis of Exome Data and Expansion to Include Studies of Additional Family Members

We previously showed in a pilot study (N = 74 families) that reanalysis in the research setting could potentially solve the previously unsolved clinical exomes for about half of affected individuals.[26] Effective experimental approaches for improving molecular diagnostic "solved rates" included: expanding singleton ES to additional family members (trio ES or other affected family member[s]) and applying additional, in-house-developed bioinformatics tools to detect indels, CNVs, and *de novo* variants with more relaxed analysis parameters. In the phase II study, we also expanded singleton ES to trio ES in ten previously studied families to uncover the genetic etiology of arthrogryposis and evaluate the diagnostic value of trio ES over singleton ES. Four out of ten families (40%) were provided with a molecular diagnosis upon expansion to trio ES and the application of bioinformatics tools to identify *de novo* and compound heterozygous variants and CNVs.[26] For the remaining ten families for whom parental samples were not available, reanalysis revealed variants that can potentially explain the molecular etiology of the observed phenotypes in five families. The overall diagnostic rate of exome reanalysis, including expansion to trio ES, in this cohort is 45% (9/20), which is consistent with our previous findings of the diagnostic utility of reanalysis.[26] Crucial experimental approaches for a reanalysis cohort are detailed in Table S4.

Phenotypic Expansion

In two personal genomes from unrelated individuals, we found variants in genes previously associated with conditions that do not include arthrogryposis as a phenotype; we now propose an expansion of the known phenotypes associated with these genes. Individual BAB7308 was found to have a *de novo*, heterozygous *SYT2* (MIM: 600104) variant (GenBank: NM_177402; c.1081G>C [p.Asp361His], Figure S8), and details of this individual are described in Tables 1 and S1 and the Supplemental Text. The second individual, BAB8356, had proband ES, which revealed a homozygous change (GenBank: NM_005245; c.6026A>G [p.Asn2009Ser]) in FAT tumor-suppressor homolog 1 - *Drosophila* (*FAT1*) (Figure S9). Clinical details of this gene are described in the Supplemental Text. Bi-allelic variants of *FAT1* were shown to cause glomerulotubular nephropathy.[61] Interestingly, two recent studies showed that *FAT1* expression has a role in the pathogenesis of fascioscapulohumeral dystrophy (FSHD1 [MIM: 158900]).[62,63] Two additional studies showed heterozygous rare variants of *FAT1* in individuals with FSHD.[64,65] FAT1 is a member of protocadherin and has a role in smooth muscle cell motility, actin accumulation, cell polarity, migrating muscle precursors, and kidney development.[66–69] We here propose another bi-allelic variant in this gene with a phenotype of arthrogryposis. Interestingly, there are increasing examples of Mendelian disease-gene discoveries for which bi-allelic variation associated with a recessively inherited trait is identified in a gene previously or simultaneously described in association with a dominant trait conferred by mono-allelic variation. *MAB21L2* (MIM: 604357), associated with dominant and recessive forms of microphthalmia/coloboma and skeletal dysplasia syndrome (MCSKS [MIM: 615877]), and *ATAD3A* (MIM: 612316), associated with autosomal-dominant or recessive Harel-Yoon syndrome (HAYOS [MIM: 617183]), are examples that illustrate both *de novo* and homozygous variants, and they lead to dominantly and recessively inherited conditions, respectively, that are associated with a single locus,[17,18] as is now described for *MFN2* (MIM: 608507), *TGFB3* (MIM: 190230), *CIT* (MIM: 605629), *SPEG*, *ADNP*, and *FAT1* in the present study.

Rare-Variant Multilocus Pathogenic Variation

In the combined phase I + phase II arthrogryposis cohort, we identified 19 families with rare variation found at more

than one locus and contributing to the observed phenotype; there were 16 individuals with an AR + AR (14 individuals) or AR + AR + AR (two individuals) multilocus disease-trait pattern, representing 84.2% (16/19) of individuals with multilocus variation (Figure 1C). Of the 37 identified AR molecular loci in all 19 individuals with multiple molecular diagnoses, 31 (31/37, 83.7%) loci demonstrated homozygosity for rare variants that are private to the studied clan (the Turkish population frequency can be found in Table S1). This is in striking contrast to an analysis of multilocus variation in a cohort of North American referrals to a diagnostic laboratory; for this cohort there were 11 individuals with an AR + AR (nine individuals) or AR + AR + AR (two individuals) disease pattern, representing 10.9% (11/101) of multilocus variation individuals studied (Figure 1C).[10] The relative frequency of multiple molecular diagnoses was higher (22%, 19/86) in the arthrogryposis cohort compared to a relatively outbred population (4.9%, 101/2076), and this was driven by a high rate of AR + AR diagnoses (84.2% 16/19) in the arthrogryposis cohort compared to the North American referral population (10.9%, 11/101, two-tailed $p < 0.0001$, Fisher's exact test). Further evidence for IBD-driven, genome-wide accumulation of deleterious variants is shown in large cohort population studies as well.[70]

In summary, we provide evidence for multiple candidate genes and further evidence for multilocus pathogenic variation that contributes to the complex trait of arthrogryposis. Moreover, we provide evidence further extending the clan genomics hypothesis[71] and emboldening the rare-variant multilocus-pathogenic-variation model for a complex trait. This study also highlights: (1) the value of reanalysis and exome variant analyses on additional family members and its ability to conclude a molecular diagnosis in this era of rapid gene discovery, (2) oligogenic inheritance and blended phenotypes can be responsible for up to ~22% of the arthrogryposis diagnoses in individuals, and the majority of this can be driven by population substructure and IBD, (3) both mono-allelic and bi-allelic variants in a single gene can contribute to human disease, causing either similar or different phenotypes, (4) paralogs of known disease-associated genes can be responsible for disease traits, and (5) genetic models for complex traits can be built from underlying Mendelian principles and explored experimentally.

Accession Numbers

The dbGaP accession number for all exome sequences reported in this paper and for which informed consent for data sharing in controlled-access databases has been provided is dbGaP: phs000711.v5.p1.

Supplemental Data

Supplemental Data can be found online at https://doi.org/10.1016/j.ajhg.2019.05.015.

Acknowledgments

The authors thank the families and their health care teams for participating in this project.

This work was supported in part by R35 NS105078 and MDA#512848 to J.R.L. and a jointly funded National Human Genome Research Institute (NHGRI) and National Heart, Lung, and Blood Institute (NHLBI) grant to the Baylor-Hopkins Center for Mendelian Genomics (UM1 HG006542). J.E.P. is supported by NHGRI K08 HG008986. D.P. is supported by the National Institutes of Health - Brain Disorders and Development Training Grant (T32 NS043124-17) and a Clinical Research Training Scholarship in Neuromuscular Disease partnered by the American Brain Foundation (ABF) and Muscle Study Group (MSG). This study is partly funded by Tubitak project number 217S675, Turkey to N.E. and B.T.. This study is partly funded by Indian Council of Medical Research, New Delhi, India with File no.: No.5/13/58/2015/NCD-III to A.S.

Declaration of Interests

Baylor College of Medicine (BCM) and Miraca Holdings have formed a joint venture with shared ownership and governance of the Baylor Genetics (BG), which performs clinical microarray analysis and clinical exome sequencing. J.R.L. serves on the scientific advisory board of the BG. J.R.L. has stock ownership in 23andMe, is a paid consultant for Regeneron Pharmaceuticals, and is a co-inventor on multiple United States and European patents related to molecular diagnostics for inherited neuropathies, eye diseases, and bacterial genomic fingerprinting. The other authors declare no conflicts of interest.

Received: December 18, 2018
Accepted: May 21, 2019
Published: June 20, 2019

Web Resources

1000 Genomes, http://www.1000genomes.org
ARIC Database, https://sites.cscc.unc.edu/aric/
BaFCalculator Browser, https://github.com/BCM-Lupskilab/BafCalculator
Cell Culture Repositories, https://ccr.coriell.org
CoNIFER, http://conifer.sourceforge.net
CoNVex, ftp://ftp.sanger.ac.uk/pub/users/pv1/CoNVex/Docs/CoNVex.pdf
DNM-Finder Browser, https://github.com/BCM-Lupskilab/DNM-Finder
ExAC Browser, http://exac.broadinstitute.org/
GeneMatcher Browser, https://genematcher.org/
gnomAD Browser, https://gnomad.broadinstitute.org/
Genotype-Tissue Expression - GTEx Portal, https://gtexportal.org/home/
HmzDelFinder Browser, https://github.com/BCM-Lupskilab/HMZDelFinder
Human-Fly Ortholog Comparison Browser, https://www.flyrnai.org/cgi-bin/DRSC_orthologs.pl
IGV, https://www.broadinstitute.org/igv/
Online Mendelian Inheritance in Man, https://www.omim.org/
NHLBI GO Exome Sequencing Project, https://evs.gs.washington.edu/EVS
STRING 10.5, https://string-db.org/

UCSC Genome Browser, https://genome.ucsc.edu
UniProt, https://www.uniprot.org/
DECIPHER, https://decipher.sanger.ac.uk/
XHMM, http://atgu.mgh.harvard.edu/xhmm/index.shtml

References

1. Hall, J.G. (2014). Arthrogryposis (multiple congenital contractures): Diagnostic approach to etiology, classification, genetics, and general principles. Eur. J. Med. Genet. *57*, 464–472.
2. Lowry, R.B., Sibbald, B., Bedard, T., and Hall, J.G. (2010). Prevalence of multiple congenital contractures including arthrogryposis multiplex congenita in Alberta, Canada, and a strategy for classification and coding. Birth Defects Res. A Clin. Mol. Teratol. *88*, 1057–1061.
3. Hall, J.G., and Kiefer, J. (2016). Arthrogryposis as a syndrome: Gene ontology analysis. Mol. Syndromol. *7*, 101–109.
4. Balta, B., Erdogan, M., Ergul, A.B., Sahin, Y., and Ozcan, A. (2017). Interstitial deletion 5p14.1-p15.2 and 5q14.3-q23.2 in a patient with clubfoot, blepharophimosis, arthrogryposis, and multiple congenital abnormalities. Am. J. Med. Genet. A. *173*, 2798–2802.
5. Carrascosa-Romero, M.C., Suela, J., Pardal-Fernández, J.M., Bermejo-Sánchez, E., Vidal-Company, A., MacDonald, A., Tébar-Gil, R., Martínez-Fernández, M.L., and Martínez-Frías, M.L. (2013). A 2.84 Mb deletion at 21q22.11 in a patient clinically diagnosed with Marden-Walker syndrome. Am. J. Med. Genet. A. *161A*, 2281–2290.
6. Lukusa, T., and Fryns, J.P. (2010). Pure de novo 17q25.3 micro duplication characterized by micro array CGH in a dysmorphic infant with growth retardation, developmental delay and distal arthrogryposis. Genet. Couns. *21*, 25–34.
7. Tabet, A.C., Aboura, A., Gérard, M., Pilorge, M., Dupont, C., Gadisseux, J.F., Hervy, N., Pipiras, E., Delahaye, A., Kanafani, S., et al. (2010). Molecular characterization of a de novo 6q24.2q25.3 duplication interrupting *UTRN* in a patient with arthrogryposis. Am. J. Med. Genet. A. *152A*, 1781–1788.
8. Bayram, Y., Karaca, E., Coban Akdemir, Z., Yilmaz, E.O., Tayfun, G.A., Aydin, H., Torun, D., Bozdogan, S.T., Gezdirici, A., Isikay, S., et al. (2016). Molecular etiology of arthrogryposis in multiple families of mostly Turkish origin. J. Clin. Invest. *126*, 762–778.
9. Todd, E.J., Yau, K.S., Ong, R., Slee, J., McGillivray, G., Barnett, C.P., Haliloglu, G., Talim, B., Akcoren, Z., Kariminejad, A., et al. (2015). Next generation sequencing in a large cohort of patients presenting with neuromuscular disease before or at birth. Orphanet J. Rare Dis. *10*, 148.
10. Posey, J.E., Harel, T., Liu, P., Rosenfeld, J.A., James, R.A., Coban Akdemir, Z.H., Walkiewicz, M., Bi, W., Xiao, R., Ding, Y., et al. (2017). Resolution of disease phenotypes resulting from multilocus genomic variation. N. Engl. J. Med. *376*, 21–31.
11. Tarailo-Graovac, M., Shyr, C., Ross, C.J., Horvath, G.A., Salvarinova, R., Ye, X.C., Zhang, L.H., Bhavsar, A.P., Lee, J.J., Drögemöller, B.I., et al. (2016). Exome sequencing and the management of neurometabolic disorders. N. Engl. J. Med. *374*, 2246–2255.
12. Balci, T.B., Hartley, T., Xi, Y., Dyment, D.A., Beaulieu, C.L., Bernier, F.P., Dupuis, L., Horvath, G.A., Mendoza-Londono, R., Prasad, C., et al.; FORGE Canada Consortium; and Care4Rare Canada Consortium (2017). Debunking Occam's razor: Diagnosing multiple genetic diseases in families by whole-exome sequencing. Clin. Genet. *92*, 281–289.
13. Posey, J.E., Rosenfeld, J.A., James, R.A., Bainbridge, M., Niu, Z., Wang, X., Dhar, S., Wiszniewski, W., Akdemir, Z.H., Gambin, T., et al. (2016). Molecular diagnostic experience of whole-exome sequencing in adult patients. Genet. Med. *18*, 678–685.
14. Yang, Y., Muzny, D.M., Xia, F., Niu, Z., Person, R., Ding, Y., Ward, P., Braxton, A., Wang, M., Buhay, C., et al. (2014). Molecular findings among patients referred for clinical whole-exome sequencing. JAMA *312*, 1870–1879.
15. Monies, D., Maddirevula, S., Kurdi, W., Alanazy, M.H., Alkhalidi, H., Al-Owain, M., Sulaiman, R.A., Faqeih, E., Goljan, E., Ibrahim, N., et al. (2017). Autozygosity reveals recessive mutations and novel mechanisms in dominant genes: Implications in variant interpretation. Genet. Med. *19*, 1144–1150.
16. Worman, H.J., and Bonne, G. (2007). "Laminopathies": A wide spectrum of human diseases. Exp. Cell Res. *313*, 2121–2133.
17. Rainger, J., Pehlivan, D., Johansson, S., Bengani, H., Sanchez-Pulido, L., Williamson, K.A., Ture, M., Barker, H., Rosendahl, K., Spranger, J., et al.; UK10K; and Baylor-Hopkins Center for Mendelian Genomics (2014). Monoallelic and biallelic mutations in *MAB21L2* cause a spectrum of major eye malformations. Am. J. Hum. Genet. *94*, 915–923.
18. Harel, T., Yoon, W.H., Garone, C., Gu, S., Coban-Akdemir, Z., Eldomery, M.K., Posey, J.E., Jhangiani, S.N., Rosenfeld, J.A., Cho, M.T., et al.; Baylor-Hopkins Center for Mendelian Genomics; and University of Washington Center for Mendelian Genomics (2016). Recurrent *de novo* and biallelic variation of *ATAD3A*, encoding a mitochondrial membrane protein, results in distinct neurological syndromes. Am. J. Hum. Genet. *99*, 831–845.
19. Warner, L.E., Mancias, P., Butler, I.J., McDonald, C.M., Keppen, L., Koob, K.G., and Lupski, J.R. (1998). Mutations in the early growth response 2 (EGR2) gene are associated with hereditary myelinopathies. Nat. Genet. *18*, 382–384.
20. Posey, J.E., O'Donnell-Luria, A.H., Chong, J.X., Harel, T., Jhangiani, S.N., Coban Akdemir, Z.H., Buyske, S., Pehlivan, D., Carvalho, C.M.B., Baxter, S., et al.; Centers for Mendelian Genomics (2019). Insights into genetics, human biology and disease gleaned from family based genomic studies. Genet. Med. *21*, 798–812.
21. Lupski, J.R., Reid, J.G., Gonzaga-Jauregui, C., Rio Deiros, D., Chen, D.C., Nazareth, L., Bainbridge, M., Dinh, H., Jing, C., Wheeler, D.A., et al. (2010). Whole-genome sequencing in a patient with Charcot-Marie-Tooth neuropathy. N. Engl. J. Med. *362*, 1181–1191.
22. Reid, J.G., Carroll, A., Veeraraghavan, N., Dahdouli, M., Sundquist, A., English, A., Bainbridge, M., White, S., Salerno, W., Buhay, C., et al. (2014). Launching genomics into the cloud: Deployment of Mercury, a next generation sequence analysis pipeline. BMC Bioinformatics *15*, 30.
23. Challis, D., Yu, J., Evani, U.S., Jackson, A.R., Paithankar, S., Coarfa, C., Milosavljevic, A., Gibbs, R.A., and Yu, F. (2012). An integrative variant analysis suite for whole exome next-generation sequencing data. BMC Bioinformatics *13*, 8.
24. Li, H., Handsaker, B., Wysoker, A., Fennell, T., Ruan, J., Homer, N., Marth, G., Abecasis, G., Durbin, R.; and 1000 Genome Project Data Processing Subgroup (2009). The Sequence Alignment/Map format and SAMtools. Bioinformatics *25*, 2078–2079.
25. Wang, K., Li, M., and Hakonarson, H. (2010). ANNOVAR: Functional annotation of genetic variants from high-throughput sequencing data. Nucleic Acids Res. *38*, e164.

26. Eldomery, M.K., Coban-Akdemir, Z., Harel, T., Rosenfeld, J.A., Gambin, T., Stray-Pedersen, A., Küry, S., Mercier, S., Lessel, D., Denecke, J., et al. (2017). Lessons learned from additional research analyses of unsolved clinical exome cases. Genome Med. *9*, 26.
27. Karaca, E., Harel, T., Pehlivan, D., Jhangiani, S.N., Gambin, T., Coban Akdemir, Z., Gonzaga-Jauregui, C., Erdin, S., Bayram, Y., Campbell, I.M., et al. (2015). Genes that affect brain structure and function identified by rare variant analyses of Mendelian neurologic disease. Neuron *88*, 499–513.
28. Gambin, T., Akdemir, Z.C., Yuan, B., Gu, S., Chiang, T., Carvalho, C.M.B., Shaw, C., Jhangiani, S., Boone, P.M., Eldomery, M.K., et al. (2017). Homozygous and hemizygous CNV detection from exome sequencing data in a Mendelian disease cohort. Nucleic Acids Res. *45*, 1633–1648.
29. Sobreira, N., Schiettecatte, F., Valle, D., and Hamosh, A. (2015). GeneMatcher: A matching tool for connecting investigators with an interest in the same gene. Hum. Mutat. *36*, 928–930.
30. Sobreira, N., Schiettecatte, F., Boehm, C., Valle, D., and Hamosh, A. (2015). New tools for Mendelian disease gene identification: PhenoDB variant analysis module; and GeneMatcher, a web-based tool for linking investigators with an interest in the same gene. Hum. Mutat. *36*, 425–431.
31. Karaca, E., Posey, J.E., Coban Akdemir, Z., Pehlivan, D., Harel, T., Jhangiani, S.N., Bayram, Y., Song, X., Bahrambeigi, V., Yuregir, O.O., et al. (2018). Phenotypic expansion illuminates multilocus pathogenic variation. Genet. Med. *20*, 1528–1537.
32. Olshen, A.B., Venkatraman, E.S., Lucito, R., and Wigler, M. (2004). Circular binary segmentation for the analysis of array-based DNA copy number data. Biostatistics *5*, 557–572.
33. Spence, J.E., Perciaccante, R.G., Greig, G.M., Willard, H.F., Ledbetter, D.H., Hejtmancik, J.F., Pollack, M.S., O'Brien, W.E., and Beaudet, A.L. (1988). Uniparental disomy as a mechanism for human genetic disease. Am. J. Hum. Genet. *42*, 217–226.
34. Gambin, T., Yuan, B., Bi, W., Liu, P., Rosenfeld, J.A., Coban-Akdemir, Z., Pursley, A.N., Nagamani, S.C.S., Marom, R., Golla, S., et al. (2017). Identification of novel candidate disease genes from de novo exonic copy number variants. Genome Med. *9*, 83.
35. Pehlivan, D., Hullings, M., Carvalho, C.M., Gonzaga-Jauregui, C.G., Loy, E., Jackson, L.G., Krantz, I.D., Deardorff, M.A., and Lupski, J.R. (2012). *NIPBL* rearrangements in Cornelia de Lange syndrome: Evidence for replicative mechanism and genotype-phenotype correlation. Genet. Med. *14*, 313–322.
36. Tsai, E.A., Grochowski, C.M., Falsey, A.M., Rajagopalan, R., Wendel, D., Devoto, M., Krantz, I.D., Loomes, K.M., and Spinner, N.B. (2015). Heterozygous deletion of *FOXA2* segregates with disease in a family with heterotaxy, panhypopituitarism, and biliary atresia. Hum. Mutat. *36*, 631–637.
37. Hu, Y., Flockhart, I., Vinayagam, A., Bergwitz, C., Berger, B., Perrimon, N., and Mohr, S.E. (2011). An integrative approach to ortholog prediction for disease-focused and other functional studies. BMC Bioinformatics *12*, 357.
38. Malfatti, E., Böhm, J., Lacène, E., Beuvin, M., Romero, N.B., and Laporte, J. (2015). A premature stop codon in *MYO18B* is associated with severe nemaline myopathy with cardiomyopathy. J. Neuromuscul. Dis. *2*, 219–227.
39. Alazami, A.M., Kentab, A.Y., Faqeih, E., Mohamed, J.Y., Alkhalidi, H., Hijazi, H., and Alkuraya, F.S. (2015). A novel syndrome of Klippel-Feil anomaly, myopathy, and characteristic facies is linked to a null mutation in *MYO18B*. J. Med. Genet. *52*, 400–404.
40. Nilipour, Y., Nafissi, S., Tjust, A.E., Ravenscroft, G., Hossein Nejad Nedai, H., Taylor, R.L., Varasteh, V., Pedrosa Domellöf, F., Zangi, M., Tonekaboni, S.H., et al. (2018). Ryanodine receptor type 3 (*RYR3*) as a novel gene associated with a myopathy with nemaline bodies. Eur. J. Neurol. *25*, 841–847.
41. Bertocchini, F., Ovitt, C.E., Conti, A., Barone, V., Schöler, H.R., Bottinelli, R., Reggiani, C., and Sorrentino, V. (1997). Requirement for the ryanodine receptor type 3 for efficient contraction in neonatal skeletal muscles. EMBO J. *16*, 6956–6963.
42. Jeyakumar, L.H., Copello, J.A., O'Malley, A.M., Wu, G.M., Grassucci, R., Wagenknecht, T., and Fleischer, S. (1998). Purification and characterization of ryanodine receptor 3 from mammalian tissue. J. Biol. Chem. *273*, 16011–16020.
43. Abath Neto, O., Tassy, O., Biancalana, V., Zanoteli, E., Pourquié, O., and Laporte, J. (2014). Integrative data mining highlights candidate genes for monogenic myopathies. PLoS ONE *9*, e110888.
44. Flix, B., de la Torre, C., Castillo, J., Casal, C., Illa, I., and Gallardo, E. (2013). Dysferlin interacts with calsequestrin-1, myomesin-2 and dynein in human skeletal muscle. Int. J. Biochem. Cell Biol. *45*, 1927–1938.
45. Helsmoortel, C., Vulto-van Silfhout, A.T., Coe, B.P., Vandeweyer, G., Rooms, L., van den Ende, J., Schuurs-Hoeijmakers, J.H., Marcelis, C.L., Willemsen, M.H., Vissers, L.E., et al. (2014). A SWI/SNF-related autism syndrome caused by de novo mutations in *ADNP*. Nat. Genet. *46*, 380–384.
46. Reinstein, E., Drasinover, V., Lotan, R., Gal-Tanamy, M., Bolocan Nachman, I., Eyal, E., Jaber, L., Magal, N., and Shohat, M. (2018). Mutations in *ERGIC1* cause arthrogryposis multiplex congenita, neuropathic type. Clin. Genet. *93*, 160–163.
47. Breuza, L., Halbeisen, R., Jenö, P., Otte, S., Barlowe, C., Hong, W., and Hauri, H.P. (2004). Proteomics of endoplasmic reticulum-Golgi intermediate compartment (ERGIC) membranes from brefeldin A-treated HepG2 cells identifies ERGIC-32, a new cycling protein that interacts with human Erv46. J. Biol. Chem. *279*, 47242–47253.
48. Knierim, E., Gill, E., Seifert, F., Morales-Gonzalez, S., Unudurthi, S.D., Hund, T.J., Stenzel, W., and Schuelke, M. (2017). A recessive mutation in beta-IV-spectrin (*SPTBN4*) associates with congenital myopathy, neuropathy, and central deafness. Hum. Genet. *136*, 903–910.
49. Anazi, S., Maddirevula, S., Salpietro, V., Asi, Y.T., Alsahli, S., Alhashem, A., Shamseldin, H.E., AlZahrani, F., Patel, N., Ibrahim, N., et al. (2017). Expanding the genetic heterogeneity of intellectual disability. Hum. Genet. *136*, 1419–1429.
50. Lange, S., Ouyang, K., Meyer, G., Cui, L., Cheng, H., Lieber, R.L., and Chen, J. (2009). Obscurin determines the architecture of the longitudinal sarcoplasmic reticulum. J. Cell Sci. *122*, 2640–2650.
51. Shin, K., Hwang, S.G., Choi, I.J., Ko, Y.G., Jeong, J., and Kwon, H. (2017). Fbxw7β, E3 ubiquitin ligase, negative regulation of primary myoblast differentiation, proliferation and migration. Anim. Sci. J. *88*, 712–719.
52. Shin, K., Ko, Y.G., Jeong, J., and Kwon, H. (2017). Skeletal muscle atrophy is induced by Fbxw7β via atrogene upregulation. Cell Biol. Int. *41*, 213–220.
53. Cheedipudi, S., Puri, D., Saleh, A., Gala, H.P., Rumman, M., Pillai, M.S., Sreenivas, P., Arora, R., Sellathurai, J., Schrøder, H.D., et al. (2015). A fine balance: Epigenetic control of cellular quiescence by the tumor suppressor PRDM2/RIZ at a

bivalent domain in the cyclin a gene. Nucleic Acids Res. *43*, 6236–6256.
54. Hodgson, B., Mafi, R., Mafi, P., and Khan, W. (2018). The regulation of differentiation of mesenchymal stem-cells into skeletal muscle: A look at signalling molecules involved in myogenesis. Curr. Stem Cell Res. Ther *13*, 384–407.
55. Carvalho, C.M., and Lupski, J.R. (2016). Mechanisms underlying structural variant formation in genomic disorders. Nat. Rev. Genet. *17*, 224–238.
56. Yang, Y., Muzny, D.M., Reid, J.G., Bainbridge, M.N., Willis, A., Ward, P.A., Braxton, A., Beuten, J., Xia, F., Niu, Z., et al. (2013). Clinical whole-exome sequencing for the diagnosis of mendelian disorders. N. Engl. J. Med. *369*, 1502–1511.
57. Böhm, J., Vasli, N., Malfatti, E., Le Gras, S., Feger, C., Jost, B., Monnier, N., Brocard, J., Karasoy, H., Gérard, M., et al. (2013). An integrated diagnosis strategy for congenital myopathies. PLoS ONE *8*, e67527.
58. Casey, W.M., Brodie, T., Yoon, L., Ni, H., Jordan, H.L., and Cariello, N.F. (2008). Correlation analysis of gene expression and clinical chemistry to identify biomarkers of skeletal myopathy in mice treated with PPAR agonist GW610742X. Biomarkers *13*, 364–376.
59. Bower, N.I., and Johnston, I.A. (2010). Discovery and characterization of nutritionally regulated genes associated with muscle growth in Atlantic salmon. Physiol. Genomics *42A*, 114–130.
60. Yamamoto, S., Jaiswal, M., Charng, W.L., Gambin, T., Karaca, E., Mirzaa, G., Wiszniewski, W., Sandoval, H., Haelterman, N.A., Xiong, B., et al. (2014). A drosophila genetic resource of mutants to study mechanisms underlying human genetic diseases. Cell *159*, 200–214.
61. Gee, H.Y., Sadowski, C.E., Aggarwal, P.K., Porath, J.D., Yakulov, T.A., Schueler, M., Lovric, S., Ashraf, S., Braun, D.A., Halbritter, J., et al. (2016). *FAT1* mutations cause a glomerulotubular nephropathy. Nat. Commun. *7*, 10822.
62. Caruso, N., Herberth, B., Bartoli, M., Puppo, F., Dumonceaux, J., Zimmermann, A., Denadai, S., Lebossé, M., Roche, S., Geng, L., et al. (2013). Deregulation of the protocadherin gene FAT1 alters muscle shapes: Implications for the pathogenesis of facioscapulohumeral dystrophy. PLoS Genet. *9*, e1003550.
63. Mariot, V., Roche, S., Hourdé, C., Portilho, D., Sacconi, S., Puppo, F., Duguez, S., Rameau, P., Caruso, N., Delezoide, A.L., et al. (2015). Correlation between low *FAT1* expression and early affected muscle in facioscapulohumeral muscular dystrophy. Ann. Neurol. *78*, 387–400.
64. Puppo, F., Dionnet, E., Gaillard, M.C., Gaildrat, P., Castro, C., Vovan, C., Bertaux, K., Bernard, R., Attarian, S., Goto, K., et al. (2015). Identification of variants in the 4q35 gene *FAT1* in patients with a facioscapulohumeral dystrophy-like phenotype. Hum. Mutat. *36*, 443–453.
65. Park, H.J., Lee, W., Kim, S.H., Lee, J.H., Shin, H.Y., Kim, S.M., Park, K.D., Lee, J.H., and Choi, Y.C. (2018). *FAT1* gene alteration in facioscapulohumeral muscular dystrophy type 1. Yonsei Med. J. *59*, 337–340.
66. Moeller, M.J., Soofi, A., Braun, G.S., Li, X., Watzl, C., Kriz, W., and Holzman, L.B. (2004). Protocadherin FAT1 binds Ena/VASP proteins and is necessary for actin dynamics and cell polarization. EMBO J. *23*, 3769–3779.
67. Cho, E., Feng, Y., Rauskolb, C., Maitra, S., Fehon, R., and Irvine, K.D. (2006). Delineation of a Fat tumor suppressor pathway. Nat. Genet. *38*, 1142–1150.
68. Hou, R., and Sibinga, N.E. (2009). Atrophin proteins interact with the Fat1 cadherin and regulate migration and orientation in vascular smooth muscle cells. J. Biol. Chem. *284*, 6955–6965.
69. Skouloudaki, K., Puetz, M., Simons, M., Courbard, J.R., Boehlke, C., Hartleben, B., Engel, C., Moeller, M.J., Englert, C., Bollig, F., et al. (2009). Scribble participates in Hippo signaling and is required for normal zebrafish pronephros development. Proc. Natl. Acad. Sci. USA *106*, 8579–8584.
70. Szpiech, Z.A., Mak, A.C., White, M.J., Hu, D., Eng, C., Burchard, E.G., and Hernandez, R.D. (2018). Ancestry-dependent enrichment of deleterious homozygotes in runs of homozygosity. bioRxiv *382721*. https://doi.org/10.1101/382721.
71. Lupski, J.R., Belmont, J.W., Boerwinkle, E., and Gibbs, R.A. (2011). Clan genomics and the complex architecture of human disease. Cell *147*, 32–43.

The American Journal of Human Genetics, Volume *105*

Supplemental Data

The Genomics of Arthrogryposis, a Complex Trait: Candidate Genes and Further Evidence for Oligogenic Inheritance

Davut Pehlivan, Yavuz Bayram, Nilay Gunes, Zeynep Coban Akdemir, Anju Shukla, Tatjana Bierhals, Burcu Tabakci, Yavuz Sahin, Alper Gezdirici, Jawid M. Fatih, Elif Yilmaz Gulec, Gozde Yesil, Jaya Punetha, Zeynep Ocak, Christopher M. Grochowski, Ender Karaca, Hatice Mutlu Albayrak, Periyasamy Radhakrishnan, Haktan Bagis Erdem, Ibrahim Sahin, Timur Yildirim, Ilhan A. Bayhan, Aysegul Bursali, Muhsin Elmas, Zafer Yuksel, Ozturk Ozdemir, Fatma Silan, Onur Yildiz, Osman Yesilbas, Sedat Isikay, Burhan Balta, Shen Gu, Shalini N. Jhangiani, Harsha Doddapaneni, Jianhong Hu, Donna M. Muzny, Baylor-Hopkins Center for Mendelian Genomics, Eric Boerwinkle, Richard A. Gibbs, Konstantinos Tsiakas, Maja Hempel, Katta Mohan Girisha, Davut Gul, Jennifer E. Posey, Nursel H. Elcioglu, Beyhan Tuysuz, and James R. Lupski

SUPPLEMENTARY INFORMATION

CLINICAL AND MOLECULAR INFORMATION FOR CANDIDATE, OLIGOGENIC, AND PHENOTYPIC EXPANSION FAMILIES

PROBABLY CAUSATIVE ARTHROGRYPOSIS GENES

RYR3

BAB7845 (Figure 2A-D)

BAB7845 is a 6 month old female who was diagnosed with arthrogryposis multiplex congenita. She had global hypotonia, facial dysmorphism including long eyelashes, right ptosis, left strabismus, thin lips, diffuse hyporeflexia and left hip dislocation. Musculoskeletal system evaluation showed contractures that were more severe in the fingers and toes and less severe in the elbows, knees and ankles (Figure 2B). Her parents were first degree cousins and she had one unaffected male sibling. Exome on the proband revealed a compound heterozygous mutation in *MYO18B* (NM_032608:c.[2879C>T];[3397C>T]:p.[Ala960Val];[Arg1133Trp]) and a homozygous variant in *RYR3* (NM_001243996:c.2486G>A:p.Arg829His). All three variants were within highly conserved regions and prediction scores were pathogenic for all three variants. The *RYR3* variant has been reported as heterozygous in 312 individuals and as homozygous in 1 individual in gnomAD. The *MYO18B* c.2879C>T variant was reported as heterozygous in 122 individuals and as homozygous in 1 individual in gnomAD and the c.3397C>T variant was reported as heterozygous in 15 individuals. Echocardiogram and spine X-ray were performed to evaluate for possible cardiomyopathy and Klippel-Feil deformity findings which were reported in *MYO18B* mutation carrier individuals.[1; 2] Echocardiogram

revealed a patent foramen ovale but no findings of cardiomyopathy, and spine X-ray showed kyphoscoliosis without Klippel-Feil anomaly.

PAED187 (Figure 2E-F)

This female proband is the second child of her unrelated healthy parents. Her sister is healthy as well. An older maternal half-sister has spastic paraplegia of the lower limbs attributed to a preterm birth and hypoxemia in the perinatal period. The remainder of the family history is unremarkable. The pregnancy was complicated by an abnormal ultrasound with bilateral club foot and echogenic intracardiac focus. She was born at term with normal anthropometric measurements. The diagnosis of bilateral club foot was confirmed; in addition she had contractures in all fingers of both hands. Conservative treatment of club feet, including tenotomy of Achilles tendon, did not resolve the severe bilateral club foot and equinus deformation. Eventually she underwent surgical intervention of equinus deformity at the age of 16 months. The finger contractures resolved well under physiotherapy. After the age of 10 months, global developmental delay became evident: the proband began crawling at 12 months, sitting at 16 months and walking unsupported at 25 months. She spoke her first words with 32 months. At the age of 3 years and one month she spoke 30 words with slurred speech. Intellectual development was also not age-appropriate. At the age of 2 years, she had repeated episodes resembling seizures over a period of four months. Multiple EEGs during this period were normal, and these episodes disappeared without treatment. Also starting at age of two years she developed an enteropathy with diarrhea up to ten times a day, which led to poor weight gain.

At the most recent examination at the age of 3 years and one month, evaluation was notable for a friendly girl with normal measurements (length -1.6 SD; weight -1.0 SD; OFC -0.4 SD). She was

able to walk short distances, but she fell frequently. Muscle weakness or other signs of muscle disease were not present, but she demonstrated muscular atrophy of the lower legs and limited movements of the feet that were caused by the surgical treatment of club feet. The fingers and all other joints did not show contractures, but fine motor skills were not age appropriate. She had dysmorphic features, such as a broad forehead, epicanthus, a broad and depressed nasal bridge, and small and abnormally spaced teeth. The fingers were small and short, as were the toes. The toe nails were dysplastic, and in addition she had 2-3 toe partial syndactyly. Extensive clinical, metabolic and genetic investigations were normal, except CGH-array analysis, which revealed a 144kb microdeletion in 6q22.31 of unknown significance. Trio exome identified compound heterozygosity for *RYR3* missense (NM_001036.3:c.2000A>G:p.Asp667Gly) and splice site donor (intron 83, c.11164+1G>A) alterations consistent with an autosomal recessive mode of inheritance [minor allele frequency (MAF) < 0.01]. Segregation analyses showed parents are heterozygous for each variant and the unaffected sister is wild type for both variants.

BAB8988 (Figure 2G-I)

BAB8988 is a 15 year old female, who was born to first degree cousin parents. She has four elder healthy siblings. At birth, she was found to have contractures in the right elbow and left wrist, and left hip dislocation which was surgically corrected at 2 years of age. On exam, she had a prominent forehead, blue sclera, high arched palate, bilateral ulnar deviation in both hands, flexion contractures in the elbows, fingers and toes, and scoliosis (Figure 2H). Diagnostic work up including a karyotype was normal. Trio exome revealed a deleterious, homozygous variant, NM_001243996:c.8939G>T:p.Arg2980Leu, in *RYR3*. This variant was reported in 19 individuals in gnomAD and 7 individuals in the Center for Mendelian Genomics (CMG) cohort as heterozygous.

MYOM2
BAB8905 (Figure 3A-C)

BAB8905 was born to a 27 year old G2P1 mother at term via standard vaginal delivery. She stayed in the newborn intensive care unit (NICU) for 10 days due to feeding problems. Birth weight was 3090 g (26^{th} percentile). She achieved head control at 2 months of life. She was not sitting unsupported by age 18 months. Parents did not report consanguinity; however they were from the same small village. The mother's first pregnancy was a spontaneous miscarriage at the 10^{th} week of gestation. Physical exam was performed at 18 months old. Growth parameters showed weight: 5.4 kg (-5.5 SD), height: 55 cm (-7.7 SD) and OFC: 41 cm (-4.1 SD). The proband had mild dysmorphic facial features including a depressed nasal root, small mouth and micrognathia. Musculoskeletal exam showed contractures in bilateral fingers and knees, bilateral hip dislocation and rocker bottom feet (Figure 3B). Cranial ultrasound at birth, ophthalmologic evaluation and hearing tests were unremarkable. Exome sequencing revealed a homozygous nonsynonymous variant in Myomesin-2, *MYOM2*, (NM_003970:c.621C>G:p.Ser207Arg). This amino acid is highly conserved throughout species and the amino acid change was predicted to be deleterious. This variant was reported 15 times in a heterozygous state in gnomAD and is not present in other public databases.

IN076 (Figure 3D-G)

We ascertained a consanguineous couple. The first pregnancy resulted in intrauterine fetal demise at four months of gestation. The second pregnancy was a preterm delivery at 28 weeks of gestation with intrauterine growth restriction (IUGR); the child succumbed to respiratory distress syndrome. The third pregnancy was a spontaneous abortion at six weeks of gestation. No fetal anomalies were documented in the first three pregnancies. The following fourth pregnancy, the

couple gave birth to a male baby weighing 1.96 kg and 43 cm in length. Antenatally, the fetus was noted to have echogenic bowel, IUGR, and dilatation of right atrium and right ventricle. Karyotype of the baby was normal. Postnatal echocardiography revealed a patent ductus arteriosus (4 mm). The baby had global developmental delay and did not achieve any developmental milestones. Eventually the baby died at six months of life. The fifth pregnancy was aborted at 24 weeks of gestation due to multiple congenital anomalies: antenatal ultrasonography at 21 weeks of gestation revealed cardiomegaly, ventricular septal defect, pulmonary valve reflux, hydrops fetalis, severe biventricular dysfunction, poor contractility, atrioventricular valve reflux and mild pericardial effusion. Following medical termination, postnatal examination was carried out in another center. The fetus weighed 575 g (normal), measured 23 cm (normal) in crown rump length, and had a head circumference of 22 cm (normal). Pleural and pericardial effusions were noted. Bilateral hypoplasia of the lungs was observed. Echocardiogram showed dilated atrium and hypertrophic ventricles. Ascites and hepatosplenomegaly were noted. Microscopic examination of fetal organs revealed calcification of the liver, brain and placenta.

The proband was the product of the sixth pregnancy. Antenatal ultrasonography at 19 weeks of gestation revealed hydrops fetalis, global myocardial hypokinesia, ascites, pleural and pericardial effusion, fetal akinesia and echogenic kidneys in the fetus. Following termination of pregnancy at 20 weeks of gestation, fetal autopsy was carried out. Fetal karyotype as well as parental karyotypes revealed a pericentric inversion of chromosome 9. A detailed postnatal evaluation including perinatal autopsy, radiographic evaluation, MRI of the brain and histopathological examination was performed. The index (male) weighed 380 g (normal), measured 23 cm (normal) in length, and had a head circumference of 18 cm (normal). The fetus had dysmorphic

facies with telecanthus, a depressed nasal bridge, microstomia and retrognathia. Generalized subcutaneous edema was noted. A short neck with protuberant abdomen was seen. Bilateral multiple joint contractures were noted across the shoulder, elbow, hip and knee joints. Bilateral pterygia were observed across the axillae (Figure 3E). Muscle mass was grossly reduced in all four limbs. On internal examination, lung hypoplasia was noted. Heart and major vessels were grossly normal. Abdominal visceral organs and intestines were normal. External and internal genitalia were normal. Brain examination revealed partial agenesis of the corpus callosum. Radiographs of the fetus showed a normal skeleton. Magnetic resonance imaging of the fetal brain was suggestive of corpus callosum agenesis which was confirmed by autopsy. Skeletal muscle (triceps), cardiac muscle (right ventricle), liver tissue, blood vessel (brachial artery), somatic nerve (radial nerve) and different parts of the brain (cerebrum, thalamus and cerebellum) were taken for histopathology examination. Hematoxylin and eosin (H&E) of all tissues and Periodic acid–Schiff (PAS) staining of liver and skeletal muscle was performed. Skeletal muscle showed perivascular and perimysial lymphocytic infiltrates on H&E stain. Lymphocytic infiltrates were also noted in the cardiac muscle and nerve as well. PAS stain was negative for both liver and skeletal muscle. No significant histopathological abnormality was noted in brain tissues. Exome sequencing of the proband revealed a stopgain variant, NM_003970:c.2797C>T:p.Gln933*, in *MYOM2* in homozygous state. This variant is seen in gnomAD in 27 individuals as heterozygotes. Another nonsynonymous homozygous missense variant NM_016381.5:c.553G>A:p.Asp185Asn in *TREX1* was noted in proband. This variant is not present in publically available databases like 1000 Genome project, gnomAD database and Exome Variant Server in homozygous or in heterozygous state. The variant c.553G>A occurs at amino acids conserved across various species. *In-silico* tools are consistent in predicting the

variant to be damaging the TREX1 protein function. However, segregation analysis was not performed for the variant. Pathogenic variants in *TREX1* are known to cause Aicardi-Goutieres syndrome 1, dominant and recessive (MIM: 225750); Chilblain lupus, autosomal dominant (MIM: 610448), Vasculopathy, retinal, with cerebral leukodystrophy, autosomal dominant (MIM: 192315) and Systemic lupus erythematosus, susceptibility to, autosomal dominant (MIM: 152700). Inflammatory myopathy is a known feature in Aicardi-Goutieres syndrome 1 and histopathological examination of multiple tissues including muscles of the proband showed inflammatory infiltrates.[3] However, inflammatory myopathy has been reported with other causes of arthrogryposis multiplex congenita.[4; 5] Calcification of basal ganglia, a characteristic feature of Aicardi-Goutieres syndrome 1, was not observed in the proband.[6] However, it was documented in the previous (5^{th}) pregnancy loss. Hence, there is possibility of a blended phenotype due to two recessive disorders in this family.

ABCA7
BAB6807-BAB6808 (Figure 4A-B)

BAB6807 and BAB6808 are two affected siblings born to a consanguineous union with a clinical diagnosis of distal SMA. Both siblings had distal contractures and DTRs were unobtainable. The older male sibling, BAB6808, additionally had DD/ID. Diagnostic work up including CPK level, *SMN1-2* gene testing and brain MRI were normal. We performed exome on both affected siblings and found three variants of interest. The female affected sibling, BAB6807, was found to have a homozygous stop gain mutation (NM_057166:c.619C>T:p.Gln207*) in the known *COL6A3* gene (Figure 4A). This variant has not been reported in the literature previously. Segregation studies showed that the remaining members of the family including the affected sibling, BAB6808, are heterozygous for the variant. Exome analysis additional showed

(NM_019112:c.5092C>T:p.Arg1698Trp) in *ABCA7*. This variant was reported in 8 individuals in gnomAD as heterozygous. BAB6808 who has additional DD/ID phenotype, was found to carry a deleterious homozygous variant (NM_015339:c.775A>C:p.Asn259His) in *ADNP*. Functional prediction scores for shared homozygous *ABCA7* and *ADNP* variant were deleterious and the affected amino acid residue was highly conserved between species. Sanger segregation showed that the parents were heterozygous and unaffected female sibling was wild type for the variant. Sanger segregation study for *ADNP* revealed that only the proband carries this variant in the homozygous state and the rest of the available relatives are heterozygous.

BAB10708 (Figure 4C-D)

BAB10708 is a 4 year old male born to healthy unrelated parents. He had an older unaffected female sibling. Anthropometric measurements at 4 years old revealed weight: 11.5 kg (-3SD), height: 91 cm (-2.7SD) and head circumference: 48 cm (5^{th} percentile). Physical examination revealed age appropriate speech and cooperation. He had down slanting palpebral fissures, high arched palate, 4x4 cm hyperpigmentation in left chest and pectus excavatum. Restrictions in bilateral wrists, knees and ankles and 2-5^{th} camptodactyly were noticed. He had right cryptorchidism which was confirmed by testicular ultrasound. Other diagnostic work up including echocardiogram, ophthalmologic evaluation, urinary ultrasound and karyotype were unremarkable. Trio exome sequencing revealed *de novo* variants in two known genes (*TPM2* and *SPEG*) and a compound heterozygous variant in *ABCA7* (Figure 4C). Both c.3076C>T and c.4045C>T residues were highly conserved through species and prediction scores were highly deleterious for both amino acid changes. *De novo* c.620_631dup non-frameshift insertion in *TPM2* is not reported in public databases. Monoallelic variants in *TPM2* cause broad spectrum of neuromuscular disorders including arthrogryposis multiplex congenita type 1, distal

arthrogryposis type 2B, nemaline myopathy type 4 and CAP myopathy type 2 (MIM: 108120, 601680, 609285 and 609285, respectively). c.9575C>A in *SPEG* is not reported in public databases however c.9575C>T was reported in two individuals in gnomAD. The region is partly conserved and the amino acid change is predicted to be deleterious by multiple prediction tools. Biallelic variants in *SPEG* are known to cause centronuclear myopathy 5 (MIM: 615959) however, we believe *de novo* variant in *SPEG* in this proband is also contributing to neuromuscular phenotype.

ERGIC1 (Figure 5)

BAB8802 is a 1 month old female who was born to first degree cousin parents. She is the first child of the parents and there are no children with similar findings in the family. The pregnancy was uncomplicated, with normal fetal movements and a normal ultrasound evaluation. She was born at term via C-section with a birth weight of 2660 g (7^{th} percentile). She was found to have *pes equinovarus* (PEV) and ulnar deviation of both hands at birth (Figure 5B). Anthropometric measurements were age appropriate: weight 3340 g (9^{th} percentile), height 51 cm (17^{th} percentile), and OFC 35 cm (9^{th} percentile). She had retromicrognathia and a capillary hemangioma covering the forehead and nose. She had normal tone and had social smile, consistent with age-appropriate development. Laboratory studies including a complete blood count and creatine phosphokinase (CPK) levels were normal. Imaging work-up including brain MRI, hip ultrasound, abdominal ultrasound, hearing screening, and spinal ultrasound were unremarkable. Echocardiogram showed a secundum type atrial septal defect (ASD) and patent foramen ovale (PFO). Trio exome showed a homozygous change in *ERGIC1* (NM_001031711:c.782G>A:p.Gly261Asp). This variant was predicted to be deleterious by all mutation prediction algorithms and the amino acid was in a highly conserved region. This variant

was reported neither in public nor in internal databases. Segregation study showed that the parents were heterozygous and the proband was homozygous as expected.

SPTBN4 **(Figure 6)**

BAB8691 was first evaluated at 13 months of age. Her parents were first cousins, once removed. Family history was notable for two deceased older siblings. The first child was male and died at 1 week of life due to respiratory problems. He had facial dysmorphic features and contractures in his hands and feet. The second child was a male individual and died at 7 months. He had lung malformation but parents do not report any contractures in his extremities. The proband had abnormal prenatal screening: she was found to have hydrocephaly on ultrasound and amniocentesis was recommended, but parents declined genetic testing. She was born at term via C-section with a birth weight of 2850 g (14^{th} percentile). She was intubated soon after birth due to respiratory distress and hospitalized for 3 months in NICU. She required a gastric tube for feeding. She developed seizures and was started on antiepileptic treatment. Her development was severely delayed and she did not achieve head control. She weighed 9340 g (33^{rd} percentile), with a length of 63 cm (-3.9SD) and OFC of 37 cm (-6.6 SD). She was hypotonic. She had dysmorphic facial features including a short neck, short nose, anteverted nares, bilateral epicanthus and microphthalmia, sparse eyelashes and a low posterior hairline. She had distal joint contractures, kyphoscoliosis and bilateral rocker bottom foot deformity. Brain MRI showed enlarged lateral ventricles. Abdominal ultrasound and echocardiogram were unremarkable. Ophthalmological evaluation revealed pale optic discs. CPK level was normal. She failed two hearing evaluations. The subject died at 2 years old due to respiratory failure. Trio exome revealed that she has a homozygous missense variant in *SPTBN4* causing NM_020971:c.6433G>A:p.Ala2145Thr in a well conserved region of the protein (Figure 6D). This variant was reported neither in the public databases nor internal databases. Prediction scores

are mostly deleterious for this variant. Sanger sequencing showed that parents are heterozygous and proband is homozygous as expected for an autosomal recessive disease trait.

MULTILOCUS PATHOGENIC VARIATION FAMILIES

FBN2-COL6A3 (Figure S6)

BAB8600 is a 15 month-old female who was born to an affected 33 year old mother (BAB8601). The parents of the proband were not consanguineous by report; the mother had 32 Mb of AOH, and the father had 28.3 Mb total AOH by BafCalculator, whereas the index did not have AOH blocks larger than 3 Mb. The index, BAB8600, had a Marfanoid habitus including a high arched palate and arachnodactyly, and mild restriction at the elbows and knees and bilateral PEV deformity. The mother was more severely affected and had additional neuromuscular findings of scoliosis and 2-5th finger camptodactyly (Figure S6). We performed trio exome and focused on shared variants between the mother and index. Novel variants in two known genes, *FBN2* and *COL6A3*, were found in the family. The variant in *FBN2* was a *de novo* missense change (NM_001999:c.4094G>C:p.Cys1365Ser) in the mother that was transmitted to the affected child. The *COL6A3* variant (NM_057167:c.367G>A:p.Val123Met) was a homozygous missense change in the mother and heterozygous in the affected child and maternal grandparents. Mutations in *FBN2* are known to cause autosomal dominant contractural arachnodactyly (MIM: 121050). Various mutations in *COL6A3* are known to cause several neuromuscular phenotypes including dominantly and recessively inherited Bethlem Myopathy 1 (MIM: 158810). Additional features in the mother, scoliosis and camptodactyly, can potentially be parsimoniously explained by her homozygosity for the identified variant in *COL6A3*.

NEB-MID1IP1 (Figure S7)

BAB8397 is an 11 year-old male born to a consanguineous marriage with multilocus pathogenic variation; rare variants were identified in one known disease gene and one candidate gene. He

had contractures in bilateral wrists, elbows, knees and 2-5th fingers with bilateral PEV. Trio exome showed a homozygous splice site variant (c.19101+5G>A) in *NEB* and a hemizygous nonsynonymous variant (NM_001098791:c.297C>G:p.Asn99Lys) in *MID1IP1* (Figure S7). Bohm *et al.* reported an infant with neonatal hypotonia, severe arthrogryposis and respiratory insufficiency who died at 10 day of life. The proband was found to have our variant, c.19101+5G>A, and nonsense variant p.Tyr1858* change. Muscle biopsy showed nemaline bodies, fiber size variability and type I fiber predominance.[7] Lethality in the subject can be explained by nonsense variant in the second allele. Segregation studies showed that parents are heterozygous for *NEB* variant and mother is heterozygous for the *MID1IP1* variant as expected with AR and X-linked Mendelian disease traits.

DRG1-TANC1-BRWD3

BAB8807 presented at age 4 years, having been born to a first degree cousin union with features of arthrogryposis including 5th finger camptodactyly and bilateral PEV, and developmental delay. He was found to have a dysplastic corpus callosum and abnormal visual evoked potentials (VEP) and electroretinogram (ERG). He had a normal echocardiogram, hearing test, and karyotype. We found three potential candidate genes: a homozygous nonsense mutation (NM_004147:c.118C>T:p.Arg40*) in *DRG1*, a homozygous missense variant in *TANC1* (NM_033394:c.2830C>T:p.His944Tyr), and a hemizygous splice site mutation in *BRWD3* (NM_153252:c.592-3T>C) which is known to cause developmental delay/intellectual disability (DD/ID) by deleterious variants (MIM: 300553). The *DRG1* variant was in a highly conserved region and not reported in public databases. The *TANC1* variant was in a highly conserved region as well, and was reported in the ExAC database 12 times in a heterozygous state, but no homozygous variation was reported. Prediction scores were damaging/disease causing by all algorithms. Segregation studies revealed that the parents were heterozygous and the proband

homozygous for both *DRG1* and *TANC1* variants, as expected for autosomal recessive disease traits; the mother was heterozygous and the proband hemizygous for the *BRWD3* variant. *DRG1*, Developmentally Regulated GTP binding protein 1, had not been shown to cause any disease phenotype previously. *DRG1* has been shown to have increased expression with feeding in Salmon fish and during myogenesis as well.[8] Expression studies showed that *DRG1* has a higher expression in fast muscle and eye which may explain the neuromuscular and eye findings in our subject.[8] Dysferlin was shown to bind alpha-tubulin and interacts with microtubules which are required for myogenesis and myotube elongation.[9] Additionally, Schellhaus *et al.* recently showed that DRG1 binds to microtubules, promotes microtubule polymerization and bundling and stabilizes them.[10] *TANC1* is not linked to any human phenotype previously. Granot-Hershkovitz *et al.* reported a female with psychomotor delay who was found to have a chromosome 2 inversion, inv(2)(p15;q24.2) disrupting the *TANC1* and *RBMS1* genes.[11] Avirneni-Vadlamudi *et al.* showed that *TANC1* is biologically relevant for myoblast fusion/development and has a critical role in rhabdomyosarcoma development as a downstream effector in the setting of the PAX-FOXO1 fusion oncoprotein.[12] Thus, we propose that homozygous missense variant in *TANC1* may explain the developmental delay and/or neuromuscular phenotype in our proband. *BRWD3* is known to cause Mental retardation, X-linked 93 (MIM: 300659) and the variant is likely contributing to proband's phenotype.

SPEG-MYOM3-CIT

BAB8532 is a 3 months old girl who presented with contractures involving the elbows, fingers and knees, as well as hip dislocations and contractures at birth. She also had DD/ID and ophthalmoplegia. The parents were not related but they were from the same small village. Trio exome sequencing revealed three candidate genes: two candidate genes and one known myopathy gene. She had a homozygous missense change,

NM_005876:c.6971T>A:p.Ile2324Asn, in *SPEG*. This region is highly conserved within orthologs and the variant was reported in 14 individuals in CMG cohort and 159 individuals in gnomAD. The *SPEG* gene was linked to centronuclear myopathy-5 (MIM: 615959). Prediction scores were deleterious by all algorithms. She was also found to have compound heterozygous variants in the Myomesin 3 gene (*MYOM3*) (NM_152372:c.1684G>A:p.Val562Ile and intronic [NM_152372.3:c.3534+56C>T]). The intronic region was highly conserved but the exonic variant, c.1684G>A, was not in a conserved region. The intronic variant was quite common and reported in 103 individuals as homozygous in gnomAD. Segregation studies for both genes revealed that the parents were heterozygous for the *SPEG* variant and heterozygous for each variant of the *MYOM3* gene. *MYOM3* has not been previously linked to any disorders. Only two studies involving 5 families have been reported for *SPEG*.[13; 14] Individuals with *SPEG* biallelic variants typically have myopathy, weakness, cardiomyopathy, and ophthalmoplegia. Our subject has muscle weakness and ophthalmoplegia. Myomesins (MYOM1, MYOM2 and MYOM3) are the principal components of the M-band that cross-link filamin-C and titin filaments in the middle of the sarcomere.[15; 16] Similar to titin, myomesin is a molecular spring whose elasticity guards the stability of the sarcomere.[17; 18] *MYOM3* is mainly expressed in intermediate fibers (type IIa) of skeletal muscle, *MYOM2* is mainly expressed in fast fibers, whereas *MYOM1* is expressed in all muscle fibers.[16] Interestingly, contractures were not a common feature in subjects with *SPEG* mutations, with the exception of a single person who was reported to have hip contractures. Thus, we believe *MYOM3* is contributing to the contracture phenotype in our subject. Our proband additionally has DD/ID which is not a feature in individuals with centronuclear myopathy-5, thus we searched for a molecular etiology for the observed DD/ID. We found a *de novo* deleterious heterozygous variant, NM_007174:c.2651A>C:p.Gln884Pro, in

CIT causing a nonsynonymous change. Biallelic variants in *CIT* have been shown to cause microcephaly and DD/ID (MIM: 617090).[19-21] We propose that the identified monoallelic *de novo* variant is likely explaining the DD/ID and microcephaly in our proband. We have previously demonstrated evidence for monoallelic mutations in disease genes associated with phenotypes segregating in a recessive mode of inheritance.

KLHL7-HOXA11-TNRC6C

BAB8688 presented at 7 months old with contractures of multiple joints. She was born at 35 weeks gestation via C-section with a birth weight of 2350 g. Pregnancy was complicated by polyhydramnios and IUGR with normal fetal movements. Anthropometric measurements at 7 months revealed height: 57 cm (-3.7 SD), weight: 4160 g (-4.3 SD) and OFC: 38.5 cm (-3.7 SD)]. Physical examination revealed hypotonia, microcephaly, failure to thrive, global developmental delay, arthrogryposis multiplex congenita, bilateral kidney stones. Parents were second degree cousins, and the proband had one healthy elder brother. Cranial ultrasound revealed hydrocephalus, echocardiogram showed a patent foramen ovale, and abdominal ultrasound displayed multiple kidney stones bilaterally. Her CPK level and routine bloodwork were unremarkable. She died at 14 months of life due to respiratory infection. Trio exome showed homozygous missense variants in *KLHL7* (NM_001031710:c.1258C>T:p.Arg420Cys) and *HOXA11* (NM_005523:c.304G>A:p.Val102Met) which are within the same AOH block. Both variants were predicted to be disease causing and embedded within highly conserved regions. The *KLHL7* variant has been previously reported in a Turkish individual.[22] Both variants were reported as heterozygous in two individuals in gnomAD. Additionally, Bruel *et al.* reported *KLHL7* mutations in Bohring-Opitz syndrome (BOS) subjects and highlighted the phenotypic similarity between cold-induced sweating syndrome (CISS3) and BOS.[23] The constellation of observed features in our proband was consistent with the BOS phenotype. This subject had an

additional homozygous missense variant in a highly conserved region in Trinucleotide repeat-containing gene 6 (*TNRC6C*) which was not previously linked to any disease (NM_018996:c.1022G>A:p.Gly341Glu). This variant was reported as disease causing by all mutation prediction algorithms. This gene is globally expressed with highest expression in brain per Genotype-Tissue Expression (GTEx) portal. Segregation studies for all three variants showed that the parents are heterozygous and the index is homozygous for the variants. TNRC6C plays a role in RNA-mediated gene silencing by micro-RNAs. This gene was not associated with any disease previously. Based on the mutation prediction scores, conservation and expression pattern, we propose that this gene may be responsible for the hydrocephalus phenotype in our proband that cannot be explained by *KLHL7*. Our subject additionally has a homozygous missense variant in *HOXA11*. Heterozygous frameshift mutation in this gene was initially linked to radioulnar synostosis with amegakaryocytic thrombocytopenia 1 in two families with AD inheritance pattern (MIM: 605432).[24] Radioulnar synostosis was a persistent feature in all mutation carriers but thrombocytopenia was not present in all affected individuals. Our subject has limited elbow movements but X-ray during the infantile period did not confirm the radioulnar synostosis. The family later declined repeat X-rays. *KLHL7* and *HOXA11* are embedded within the same region of AOH, and we propose that *KLHL7*, and potentially also *HOXA11*, are contributing to the observed phenotype.

ECEL1-FLII

BAB7710 is a 5 years old male, born at 28 weeks' gestation via C-section due to preterm labor with a birth weight of 2750 g. His parents were first degree cousins, and he is their only child; family history is notable for maternal cousins described as having a similar condition. The proband has down-slanting palpebral fissures, right congenital ptosis, contractures in all joints, severe kyphoscoliosis and cryptorchidism. He is tracheostomy-dependent. Echocardiogram and

abdominal ultrasound were normal. EMG/NCS showed myopathic changes and fibrosis. He was initially diagnosed with Escobar syndrome and *CHRNG* mutation screening was inconclusive. The index underwent exome sequencing which revealed two potential candidates. He had a homozygous frameshift variant in exon 2 of the *ECEL1* gene (NM_004826.3: c.505_529del;p.Gly169Serfs*26) and a homozygous nonsynonymous change (NM_001256265:c.2590C>T:p.Arg864Trp) in Flightless I Drosophila Homolog (*FLII*). This amino acid was highly conserved throughout orthologs. The *ECEL1* frameshift variant has been reported in only one individual as heterozygous in gnomAD, and the *FLII* variant has not been reported in any of the publicly available and internal databases. All computational tools predicted the *FLII* variant to be disease causing. Sanger PCR confirmed that both parents are heterozygous, and proband is homozygous for both variants. Deleterious changes in *ECEL1* are known to cause distal arthrogryposis type 5D (MIM: 615065), and it is the second most common mutated gene within our cohort. Our variant was not previously reported in subjects with *ECEL1* mutation. *FLII* is not linked to any human phenotype. It is globally expressed but highest expression is in the muscle tissue. *FLII* encodes a protein with a gelsolin-like actin binding domain and an N-terminal leucine-rich repeat-protein protein interaction domain which is similar to a Drosophila protein involved in early embryogenesis and the structural organization of indirect flight muscle. *TRPV4* which is a known gene for distal nonprogressive SMA, and present in one person within our cohort, mediates Ca^{+2} influx through interaction with fliI and non-muscle myosin IIA in fibroblast cell culture.[25] Naganawa and Hirata studied zebrafish mutants and showed that Zebrafish flii mutants show normal behavior at 24 hours but slow swimming at 48 hour through a mechanism involving actin disorganization in fast muscle fibers.[26] Campbell *et al.* constructed Flii -/- mice and demonstrated early embryonic lethality for the knockout; heterozygous carriers

did not have a detectable phenotype.[27] Since mutations in *ECEL1* are known to cause distal arthrogryposis and our proband has much more severe phenotype than would be expected, we propose that *FLII* is likely contributing to the disease phenotype.

GBE1- AP4M1-TAF9B

We found 3 potential candidate variants in BAB8400 that may explain the proband's phenotype. The proband was evaluated at age 3 years 8 months of age due to hypotonia, global developmental delay, muscle atrophy, arthrogryposis multiplex and cryptorchidism. Muscle biopsy revealed severe atrophy of type 2 fibers. Exome of the proband showed several potential disease causing candidates including homozygous nonframeshift deletion (NM_000158.3:c.1864_1866del:p.Leu622del) in the *GBE1* gene, a homozygous change (NM_004722:c.136C>G:p.Pro46Ala) in *AP4M1* and a hemizygous missense variant in *TAF9B* (NM_015975:c.133C>A:p.Arg45Ser). None of the homozygous variants in *GBE1*, *AP4M1* and *TAF9B* were reported as homozygous/hemizygous in internal and public databases. Functional prediction scores were deleterious for all variants. Segregation studies were consistent with the observed disease trait, homozygous for recessive conditions (*GBE1* and *AP4M1*) and hemizygous for X-linked recessive condition (*TAF9*). *GBE1* is known to cause glycogen storage disease, type IV which can present with neuromuscular features (MIM: 232500). Our mutation was not previously reported in the literature. Individuals with *GBE1* mutations frequently have other features of glycogen storage disorder such as cardiac and liver involvement. However, there is a recent report of a 3 years old male who presented with arthrogryposis, motor developmental delay and rigid spine who was found to have compound heterozygous mutations in *GBE1*.[28] *TAF9B* has not been linked to any human disease, however it interacts closely with *TAF6* in which deleterious variants are known to cause Alazami-Yuan syndrome, characterized by DD/ID (MIM: 617126).[29; 30] Moreover, it has been shown to regulate neuronal gene

expression.[31] Thus, we here propose that variant in *TAF9B* is contributing to the DD/ID phenotype in our proband. Mutations in *AP4M1* are known to cause Spastic Paraplegia type 50 (MIM: 612936). Although our subject has overlapping features such as DD/ID and club feet, he did not exhibit the classical hyperreflexia and spasticity phenotypes observed in spastic paraplegia. Thus it is difficult to determine the contribution of the *AP4M1* variant to the disease phenotype.

COG6-MED27

BAB8606 is a 17 day old female with had medically complicated family history. Parents were first degree cousins and she had three female siblings who died ages between 3 days of life to 3 months of life with similar features including polyhydramnios, contractures and cataract. Another female sibling with pontocerebellar hypoplasia and cataract died at 9 years old. She has a 21 year old living, male sibling, BAB8609, who has developmental delay, ataxia, dysmetria, mild contracture in knees and in wrists and bilateral cataract. Brain MRI of this sibling, BAB8609, also showed cerebellar hypoplasia. Index, BAB8606, was born at 38th gestational week with a birth weight of 2200 g (-2.3 SD) after a pregnancy complicated by polyhydramnios. She developed respiratory distress after birth. She was found to have contractures in both hands and feet and bilateral cataract. Head ultrasound showed hydrocephaly. We performed quadruple exome in this family and found a homozygous frameshift variant (NM_001145079.1:c.726del:p.Cys242Trpfs*7) in *COG6* which is linked to congenital disorder of glycosylation (CDG), type III (MIM: 614576) and Shaheen syndrome (MIM: 615328). Segregation studies showed that parents and living sibling carries this variant in heterozygous state and proband is homozygous. The gross features of this syndrome are microcephaly, DD/ID, liver involvement, recurrent infections, early lethality and hypohydrosis.[32] Cerebellar hypoplasia, early lethality and contractures are well-known clinical features of other CDG phenotypes. Our

family has multiple individuals who died early in the life and cerebellar hypoplasia in some individuals. Since our proband was evaluated at 17 day of life, we could not evaluate the typical features of CDG. Since both siblings carry additional similar clinical features including bilateral cataract, and DD/ID phenotype, we searched for shared variants in both siblings. A deleterious homozygous missense (NM_001253881:c.770C>T:p.Pro257Leu) variant in Mediator Complex Subunit 27 (*MED27*) is found in both siblings. c.770C>T variant is called to be disease causing by all mutation prediction tools, embedded in highly conserved region and not reported in any of the public databases or our internal database except within the family. Mediator Complex Subunit genes are well known to cause DD/ID phenotype, cerebellar anomalies and various eye findings.[33] *MED17* mutations are known to cause microcephaly, DD/ID and cerebellar atrophy (MIM: 613668), *MED25* mutations are known to cause Basel-Vanagait-Smirin-Yosef syndrome (MIM: 616449) which is characterized by DD/ID, various brain malformations and eye malformations including cataract. Thus, we here propose *MED27* variant is likely contributing DD/ID, cerebellar and eye findings in our siblings and more severe DD/ID and multiple early deaths among siblings can be explained by *COG6* homozygous frameshift mutation and other potential variants in other genes.

POSSIBLY CAUSATIVE ARTHROGRYPOSIS GENES

***CACUL1* (Figure S5)**

BAB9729 is a 3.5 months old male who was found to have bilateral hydronephrosis during the prenatal period. He was found to have contractures in both hands and feet at birth and diagnosed with amyoplasia congenita. Neonatal testing confirmed the prenatal diagnosis of hydronephrosis and demonstrated bilateral vesicoureteral reflux and end stage renal disease. His parents were first degree cousins, and he has two healthy siblings. He had dysmorphic facial features including a prominent forehead, hypotelorism, a long philtrum, thin lips, retromicrognathia and

low set ears. Growth parameters revealed he is small in all parameters: weight 3 kg (-4.1 SD), height 55.5 cm (-2.3 SD), and head circumference 36 cm (-3.2 SD). Head CT, karyotype and array-CGH were normal. Trio exome revealed a homozygous 2 bp deletion in a candidate gene, *CACUL1*, causing (NM_153810:c.910_911del:p.Leu304Ilefs*3) (Figure S5). This gene was not previously linked to any disease. Segregation studies showed that the parents are heterozygous, and the proband is homozygous for the deletion.

FGFRL1 **(Figure S3)**

BAB3944 is a 3 year old female, born to consanguineous parents, who first presented at the age of 6 months. She had myopathic facies, dolicocephaly, and contractures in the fingers and knees (Figure S3). She had a normal karyotype and echocardiogram. Exome sequencing initially did not reveal any candidate gene but re-analysis showed a homozygous nonsynonymous change in the *FGFRL1* gene (NM_001004356:c.124C>T:p.Arg42Trp). This amino acid is conserved in orthologs, and the variant was evaluated as disease causing in all functional prediction algorithms. This variant was present in only one individual in our internal BHCMG database and one individual in gnomAD in the heterozygous state. Segregation studies revealed that both parents and the unaffected brother are heterozygous for the variant, consistent with an autosomal recessive disease trait.

TMEM214 **(Figure S4)**

BAB5192 was first evaluated at age 2 years 4 months old with chief complaints of restricted joint movements, motor developmental delay and respiratory distress. She was born at 34 weeks and 1 day gestation by C-section. Physical examination revealed myopathic facies, scoliosis, and contractures in the shoulders, elbows, hips and knees with absent deep tendon reflexes. She was born to a first degree cousin marriage. The mother reported three miscarriages, one affected male child who died at the age of 2 with similar clinical features, one female child who died 4 day of

life of unknown clear etiology and one healthy female sibling. Diagnostic work up including blood chemistry and metabolic profile, CPK level, cranial and abdominal ultrasound, cranial MRI, congenital disorder of glycosylation testing, proband and parental karyotypes, and SMA gene testing were unremarkable. EMG/NCS was consistent with diffuse anterior horn cell disease. The proband died at 2 years 6 months of age due to respiratory complications. Exome sequencing of the proband revealed a homozygous missense change (NM_001083590:c.764G>A:p.Arg255Gln) in the *TMEM214* gene. This variant was reported in only one person in our internal database and three individuals in gnomAD as a heterozygous variant. The amino acid was present in a highly conserved region and prediction scores reported it as a disease-causing variant (Figure S4). Sanger sequencing from the available relatives showed that the father is heterozygous and the proband is homozygous, consistent with a recessive disease trait.

NR2C1

BAB8086 and BAB8087 are two affected siblings born to a first degree cousin marriage. BAB8086 is a 14 years old male and BAB8087 is a 9 years old female. Both siblings had normal growth parameters and intellectual development. They developed hirsutism and arthrogryposis after infancy. Diagnostic work up including CPK level, karyotype, EMG/NCS and brain MRI were normal. Exome sequencing was performed on two affected siblings. Exome analysis revealed a homozygous splicing variant in a highly conserved region in the *NR2C1* gene (NM_003297:c.544+1G>C). This variant was not reported in public databases. *NR2C1*, nuclear receptor subfamily 2 group C member 1, is the only convincing gene that is homozygous in both affected individuals. *NR2C1* is an orphan nuclear receptor and belongs to the nuclear hormone receptor family. It is globally expressed and together with NR2C2, forms the core of the DRED (direct repeat erythroid-definitive) complex that represses embryonic and fetal globin

transcription. Lee *et al.* recently showed its role in erythroid cell proliferation and maturation.[34] Interestingly, a homozygous knock-out mice model did not survive beyond embryonic day 7, however heterozygous animals showed increased expression of cyclin dependent kinase inhibitor (*Cdkn1c*). *CDKN1C* deleterious variants are known to cause developmental disorders including Beckwith Wiedemann syndrome and IMAGE syndrome (MIM: 130650 and 614732, respectively). Our probands have unique clinical features such as hirsutism and contractures that developed after infancy and which are atypical for classical arthrogryposis phenotypes. Given the pathogenicity of the variant, conservation and segregation studies, we propose *NR2C1* as disease causing in this family.

PRDM2 **(Figure 7)**

BAB9309 was born to a 29 year old G4P3A1 mother via normal spontaneous vaginal delivery at term. Parents were first degree consanguineous and she has two healthy siblings. Birth weight was 2390 g (-2 SD) and head circumference 30 cm (-3.3 SD). Intrauterine fetal movements and ultrasounds were unremarkable. She was consulted due to small for gestational age, microcephaly, contractures and dysmorphic features. Evaluation at 7 day of life revealed she has weak cry, bulbous nose, low set ears, micrognathia, contractures in fingers and rocker-bottom feet. Anthropometric measurements showed weight 2350 g (-2.3 SD), height 44 cm (-2.9 SD) and head circumference 30.5 cm (-3.3 SD). She failed with the initial hearing screening test. Trio exome revealed a *de novo* frameshift deletion (NM_012231:c.4283_4295del:p.Leu1428Glnfs*15) in *PRDM2* in a highly conserved region (Figure 7). Based on variant read/total read ratio (12/150=~8%), mosaicism is suspected. Sanger PCR did not show the variant thus, we conveyed ddPCR which showed mosaic *de novo* indel in the proband.

PHENOTYPIC EXPANSION

SYT2 (Figure S8)

BAB7308 is an 8 month old male born at term with via C-section with a birth weight 3600 g (53rd percentile). Mother reports decreased fetal movements during pregnancy. He was born to unrelated parents and has two healthy female siblings. He had delayed motor milestones. Physical examination showed contractures in fingers, bilateral PEV deformity and undescended testicles. Diagnostic work up including EEG and abdominal ultrasound were unremarkable however brain MRI showed partial corpus callosum agenesis and EMG/NCS was consistent with sensorimotor polyneuropathy. Ophthalmologic evaluation showed megalocornea (Figure S8). Proband exome was inconclusive thus expanding to trio exome revealed a *de novo* missense change (NM_177402:c.1081G>C:p.Asp361His) in Synaptotagmin 2 (*SYT2*) through our DNM-finder tool.[35] *SYT2* mutations have been described in two families with congenital presynaptic Myasthenia (MIM: 616040).[36] Based on functional studies[37; 38] and strong association between presynaptic Myasthenia syndrome genes and arthrogryposis (*e.g. CHRNA1* and *CHRND* mutations are known to cause both phenotypes), we propose that this family represents an expansion of the known phenotype of *SYT2* to include arthrogryposis. We could not identify any other gene/s that can explain the DD/ID, partial corpus callosum agenesis and megalocornea phenotype.

FAT1 (Figure S9)

BAB8356 is a 5 month old male born to a first degree cousin marriage. He was born term after an uncomplicated pregnancy. He was found to have a webbed neck and contractures involving both hands. Additionally he had a large fontanel, thick lips and cleft palate. Eye exam and genitourinary ultrasound were unremarkable. Skeletal survey revealed elongated metaphysis and flat vertebral bodies. Echo showed mild pulmonary stenosis. Exome sequencing of the proband

revealed a homozygous nonsynonymous change, NM_005245:c.6026A>G:p.Asn2009Ser in *FAT1* (Figure S9). This variant was reported in heterozygous state in the heterozygous state in 15 individuals from the gnomAD database and not reported in other public databases nor our internal cohort. Sanger segregation showed that the parents are heterozygous for the variant, which is consistent with an autosomal recessive Mendelian trait.

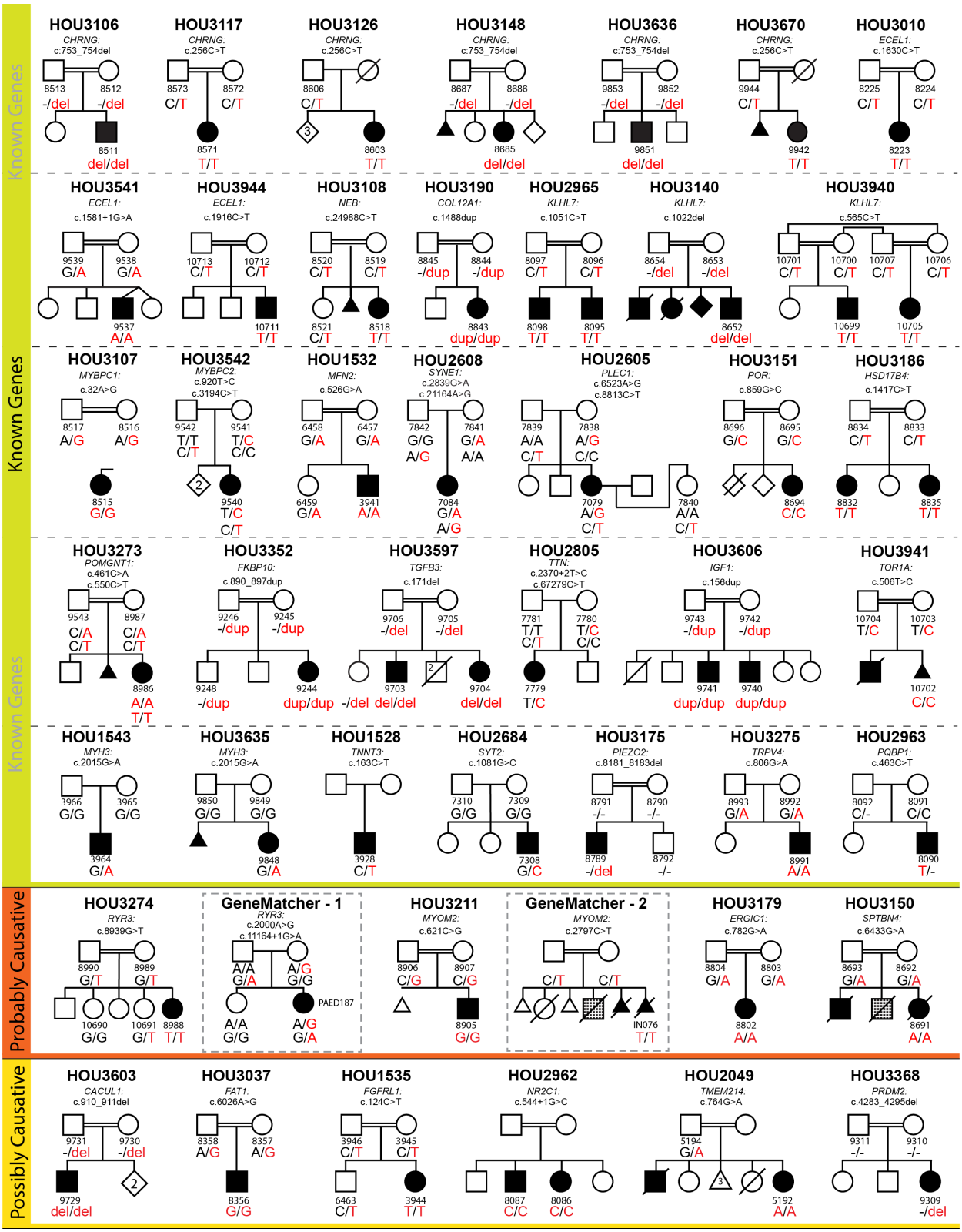

Figure S1: Pedigrees and Sanger confirmed genotypes of the known and proposed candidate gene families.

Figure S1: Pedigrees and Sanger confirmed genotypes of the known and proposed candidate gene families. Family IDs (HOU#) are written above each pedigree; filled circles (females) and squares (males) with clinical diagnosis of arthrogryposis. Genotypes are shown below each individual. Mutations are written in red, whereas wild type alleles are written in black. Subject numbers (BAB) are written under each individual whose samples were available. GeneMatcher families in probably causative genes are framed with a dashed line.

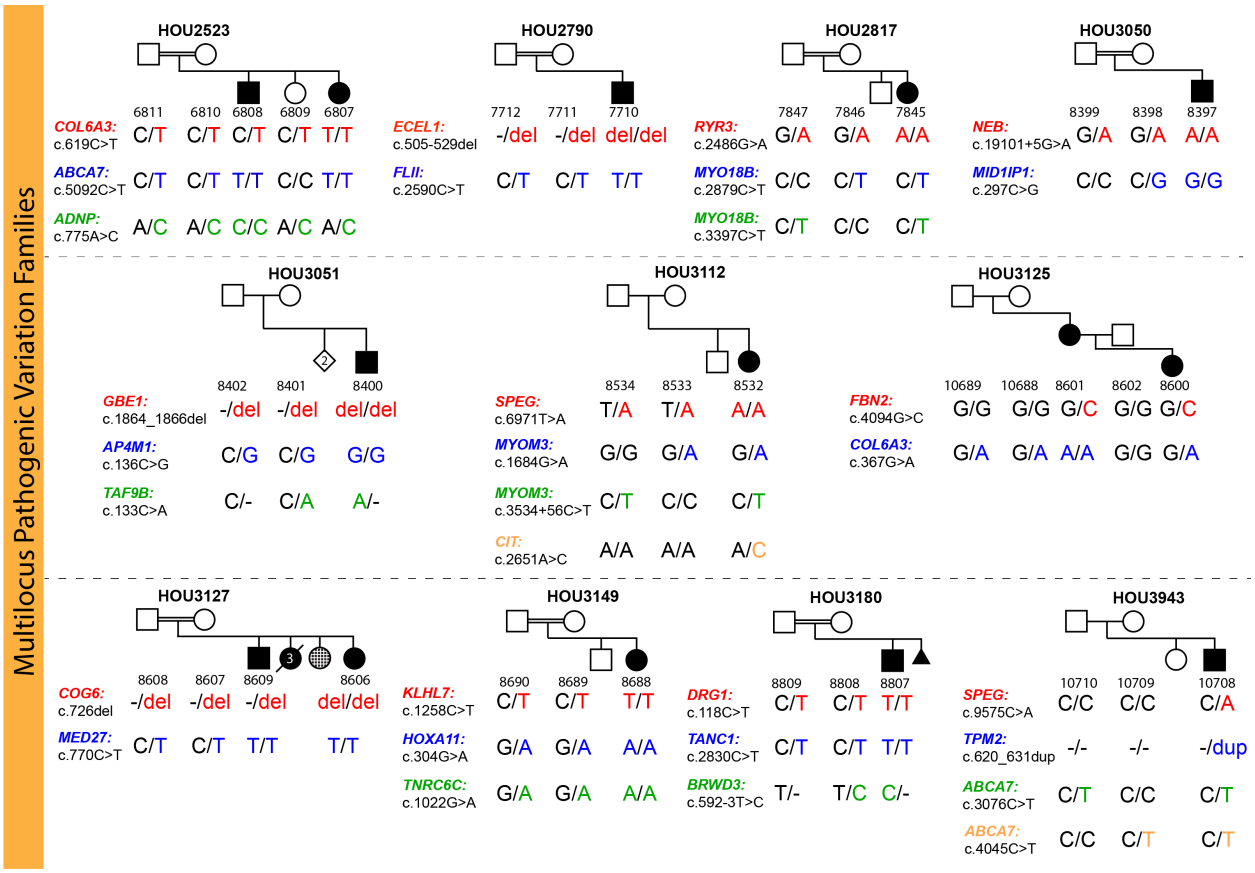

Figure S2: Segregation studies of the families with multilocus pathogenic variation. Family identification numbers are displayed on top of each pedigree. Genotypes for each variant are written in columns with each row for the given gene locus specified. BAB numbers indicating the studied subject are displayed under each shape.

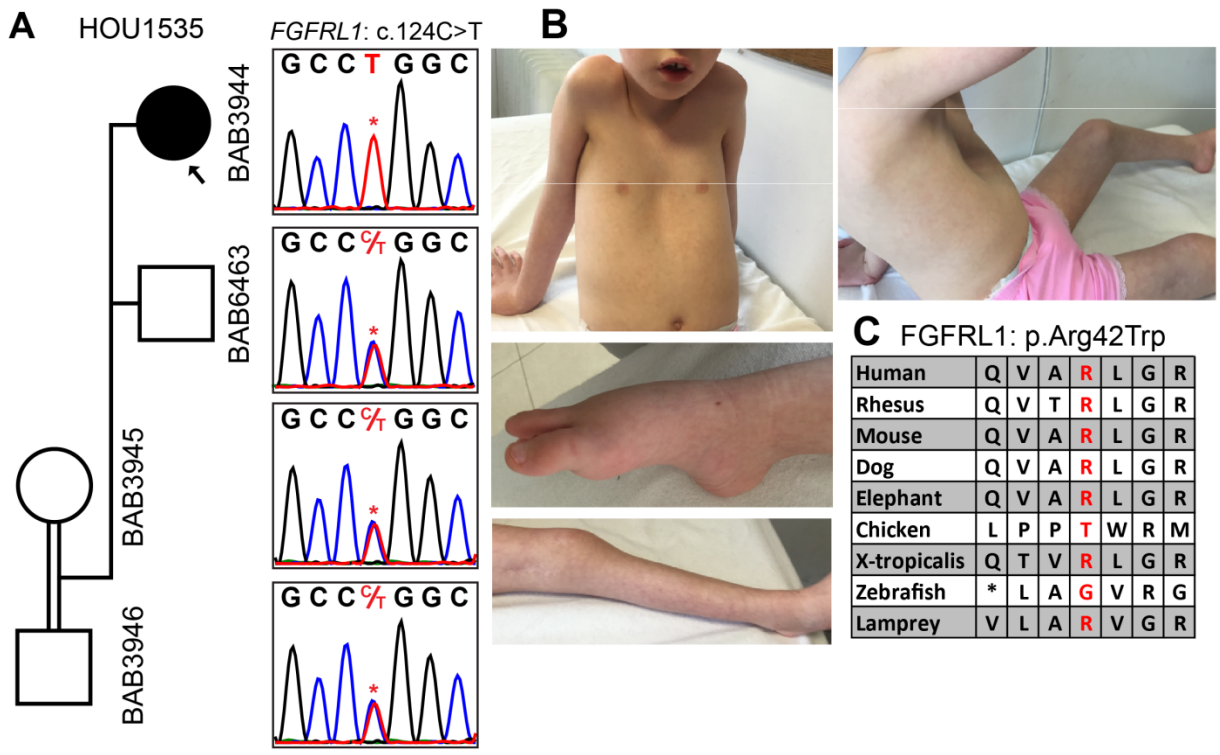

Figure S3: Pedigrees and Sanger validation of the identified variant in BAB3944. (A): Homozygous c.124C>T variant in *FGFRL1* is segregating within the family consistent with recessive Mendelian traits, *i.e.* parents and unaffected brother is heterozygous and the proband is homozygous. (B) Photographs showing contractures in hands and knees, and *pes equinovarus* deformity. (C) Highly conserved amino acid residue across different species at position 42.

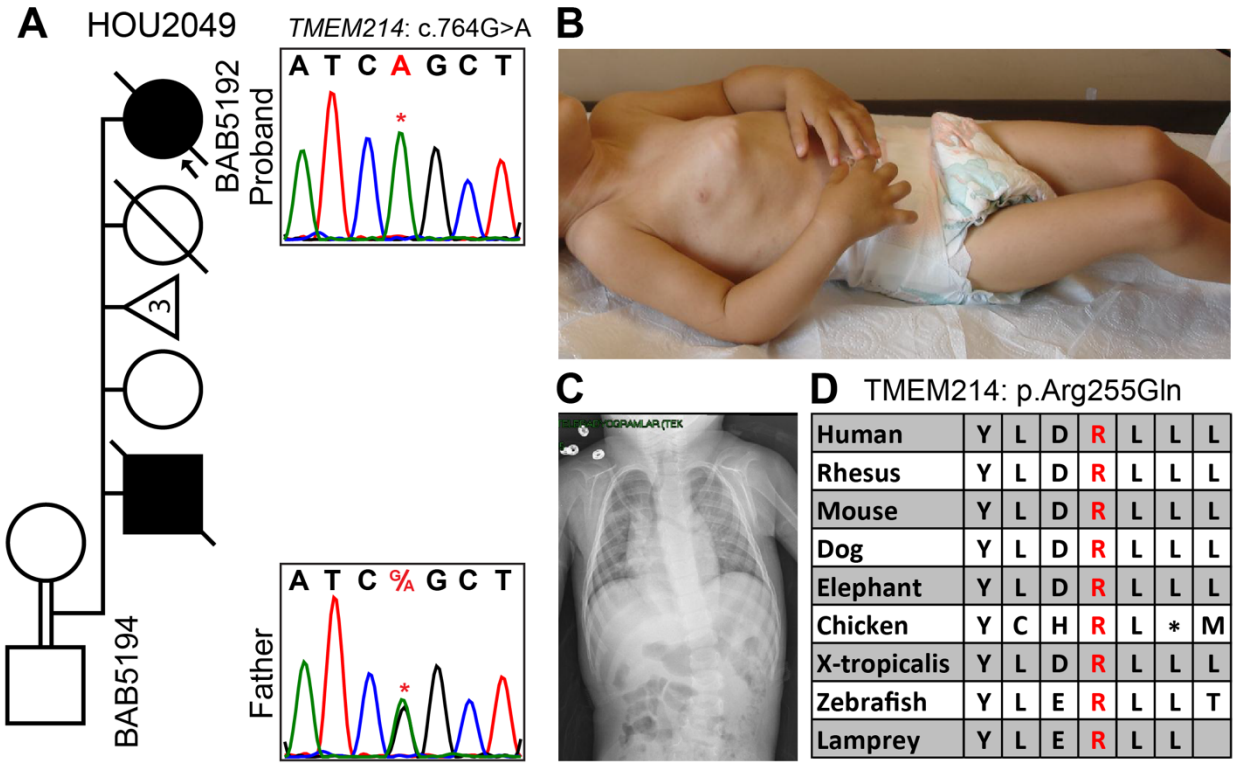

Figure S4: Details of homozygous *TMEM214* variant in BAB5192. (A) Pedigree and Sanger chromatographs of the family for segregation analyses. Affected individual has homozygous mutation whereas unaffected father is heterozygous. Mother was not available for segregation studies. (B) Picture showing contractures in shoulders, elbows, hip and knees. (C) Spinal X-ray showing scoliosis in the proband. (D) Conserved Arg (R) residue at position 255 with red font color.

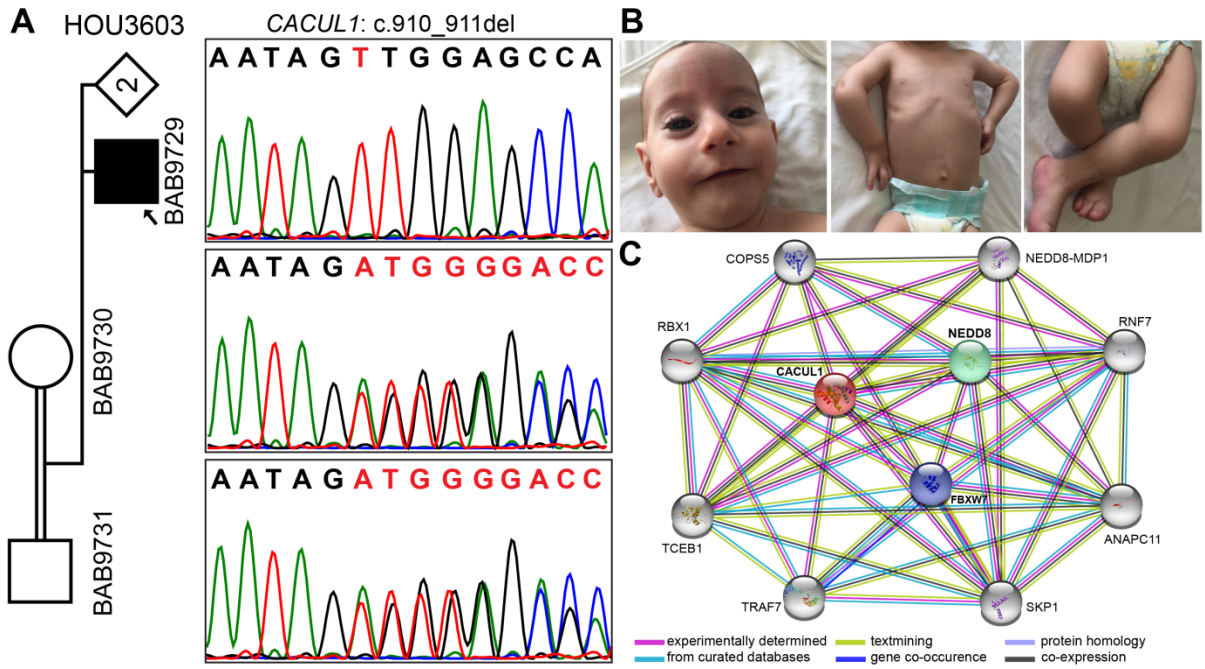

Figure S5: Clinical and molecular findings in subject with *CACUL1* variant. A) Segregation analyses of the homozygous *CACUL1* homozygous deletion in the family HOU3603. Note the peak on peak appearance on the heterozygous parents. (B) Proband's pictures showing contracture in the elbows and fingers. (C) The interaction network of *CACUL1* (green circle) with genes which have role in muscle function (blue circles). Gray circles indicate the proteins in the same network with no known neuromuscular function/phenotype. Interactome diagram is obtained through the STRING database, version 11.0. Each colored line between proteins indicates the source of the association and is indicated directly under the panel.

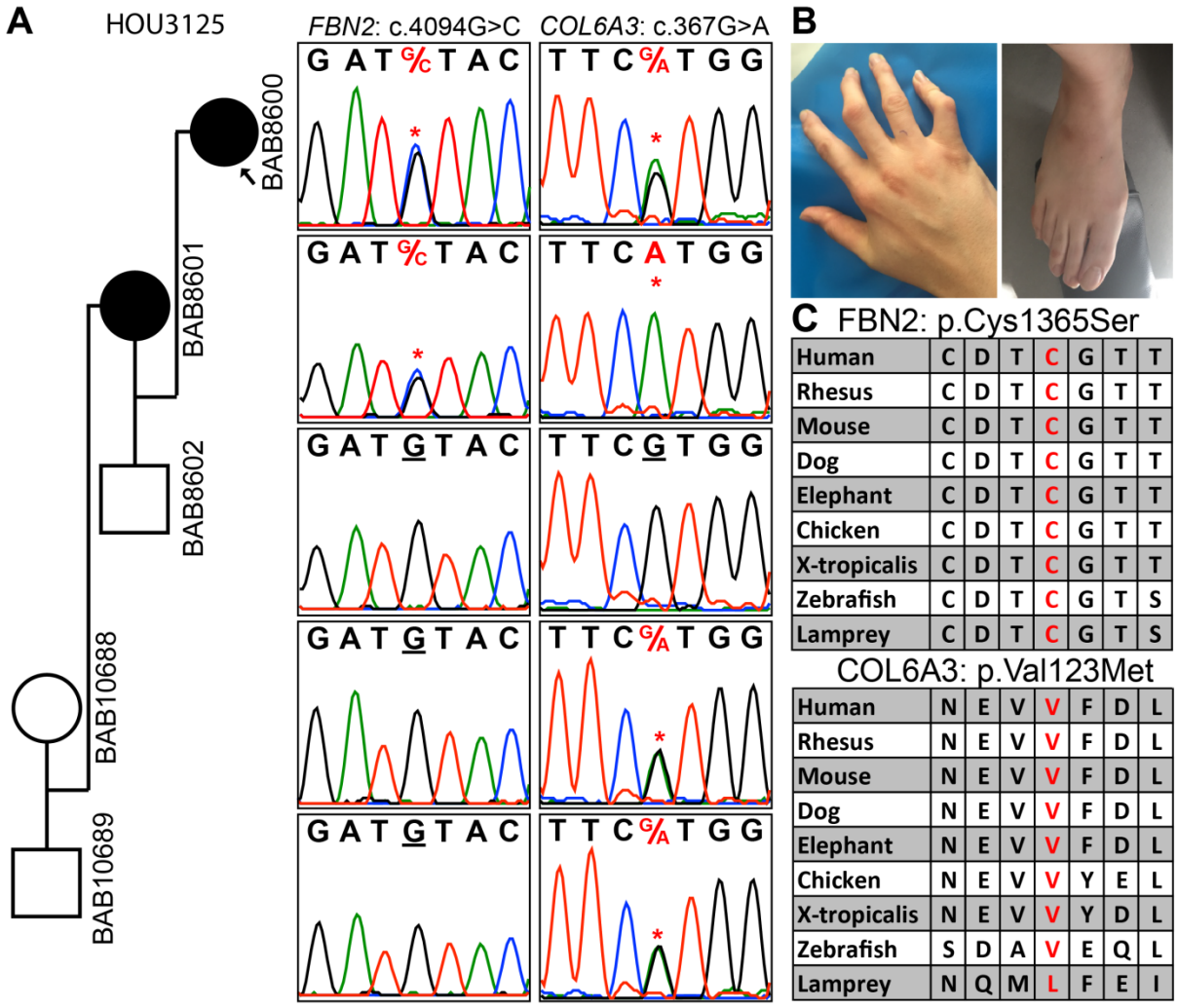

Figure S6: Known - known oligogenic model: heterozygous *FBN2* variant identified in BAB8600 and BAB8601 and a homozygous *COL6A3 variant* in the mother. (A) Sanger sequencing studies showing *de novo* heterozygous *FBN2* variant (c.4094G>C) in mother which was shared with affected daughter and a homozygous *COL6A3* variant (c.367G>A) in affected mother who has additional contractural features. Mother's affected daughter and grandparents are heterozygous for the *COL6A3* variant. (B) Photographs of the contractural arachnodactyly in fingers and toes in mother. (C) High conservation of the mutation amino acid residue for both *FBN2* and *COL6A3* variants

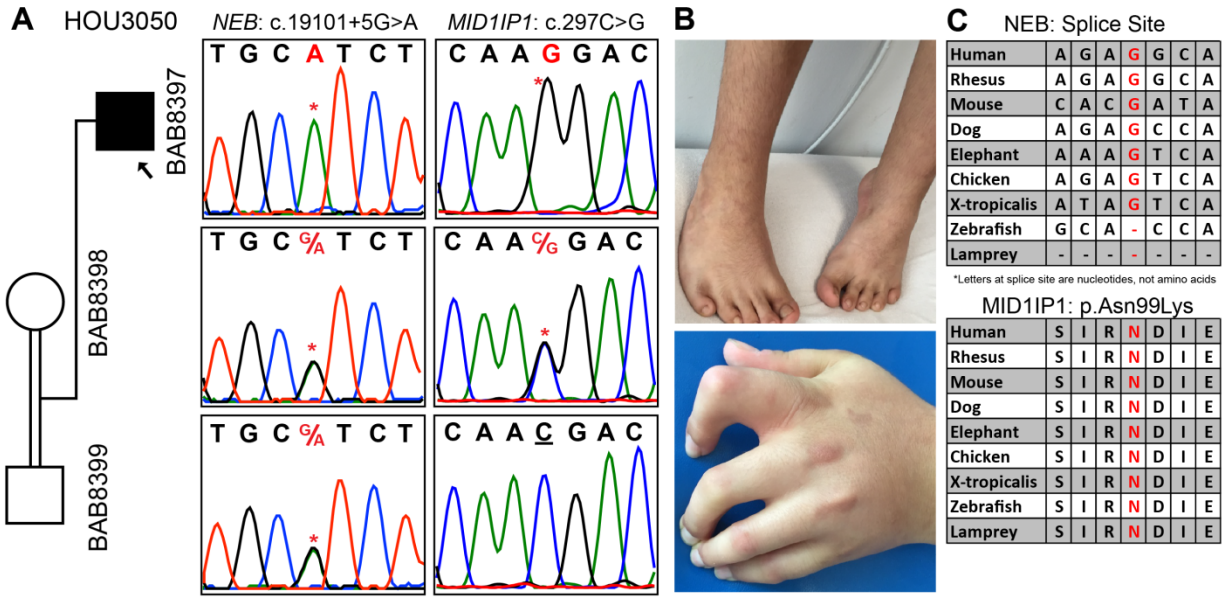

Figure S7: Known – candidate oligogenic model: Reported splice site mutation in the known *NEB* gene and missense mutation in the candidate *MID1IP1* gene. (A) Segregation analyses showing *NEB* variant (c.19101+5G>A) and a homozygous *MID1IP1* variant (c.297C>G) in the proband. Both parents are heterozygous as expected with consanguineous marriages. (B) Pictures of the proband showing contractures in fingers and *pes equinovarus* deformity in feet. (C) Conservation table for the peptide residues around *NEB* and *MID1IP1* variants.

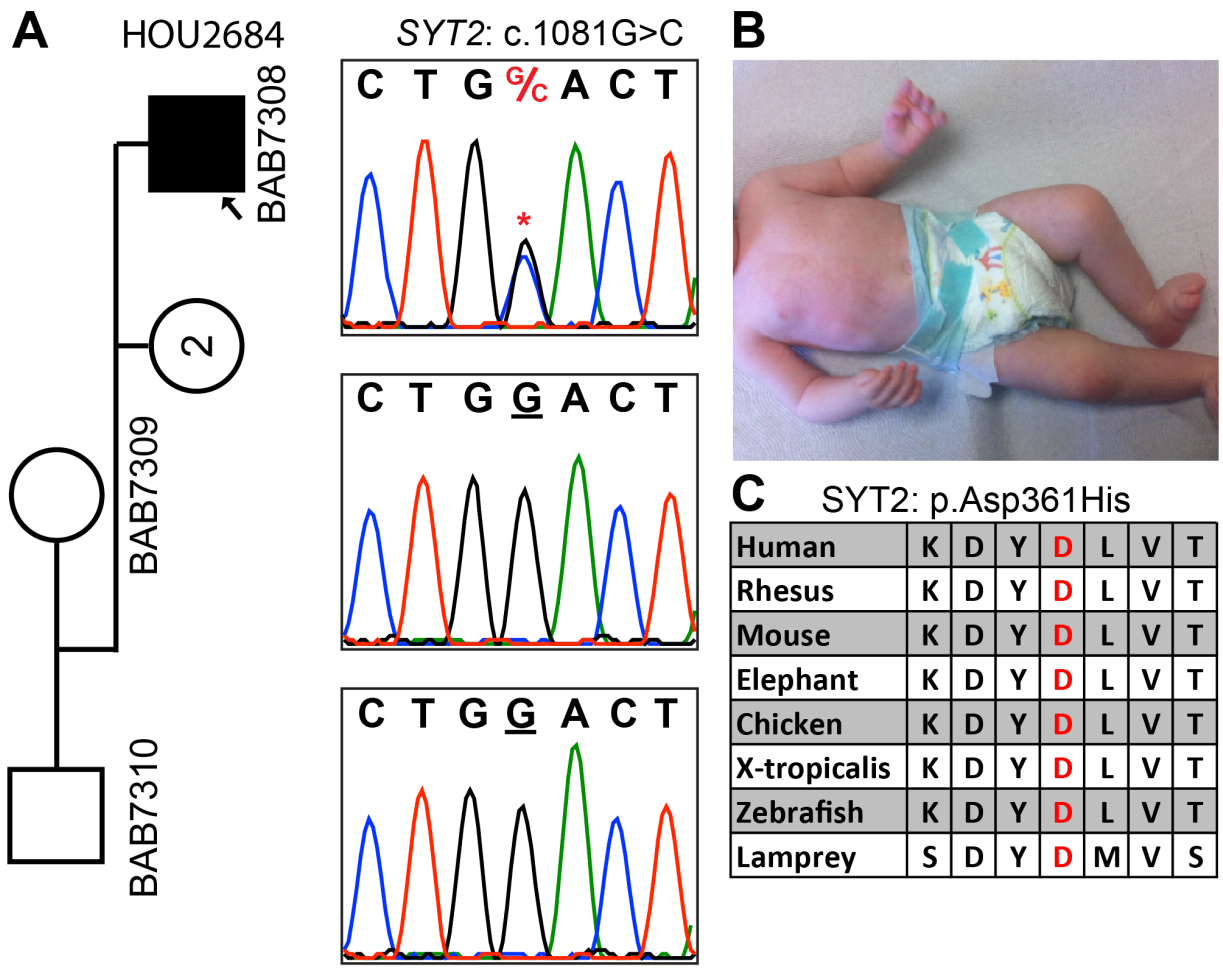

Human	K	D	Y	D	L	V	T
Rhesus	K	D	Y	D	L	V	T
Mouse	K	D	Y	D	L	V	T
Elephant	K	D	Y	D	L	V	T
Chicken	K	D	Y	D	L	V	T
X-tropicalis	K	D	Y	D	L	V	T
Zebrafish	K	D	Y	D	L	V	T
Lamprey	S	D	Y	D	M	V	S

Figure S8: *De novo* heterozygous *SYT2* variant in BAB7308. (A) Pedigree and segregation analyses of the c.1081G>C variant. (B) Proband's photographs showing the contractures in the hands and feet. (C) High conservation of Asp361His peptide in other species. Asp (D) amino acid is written in red font.

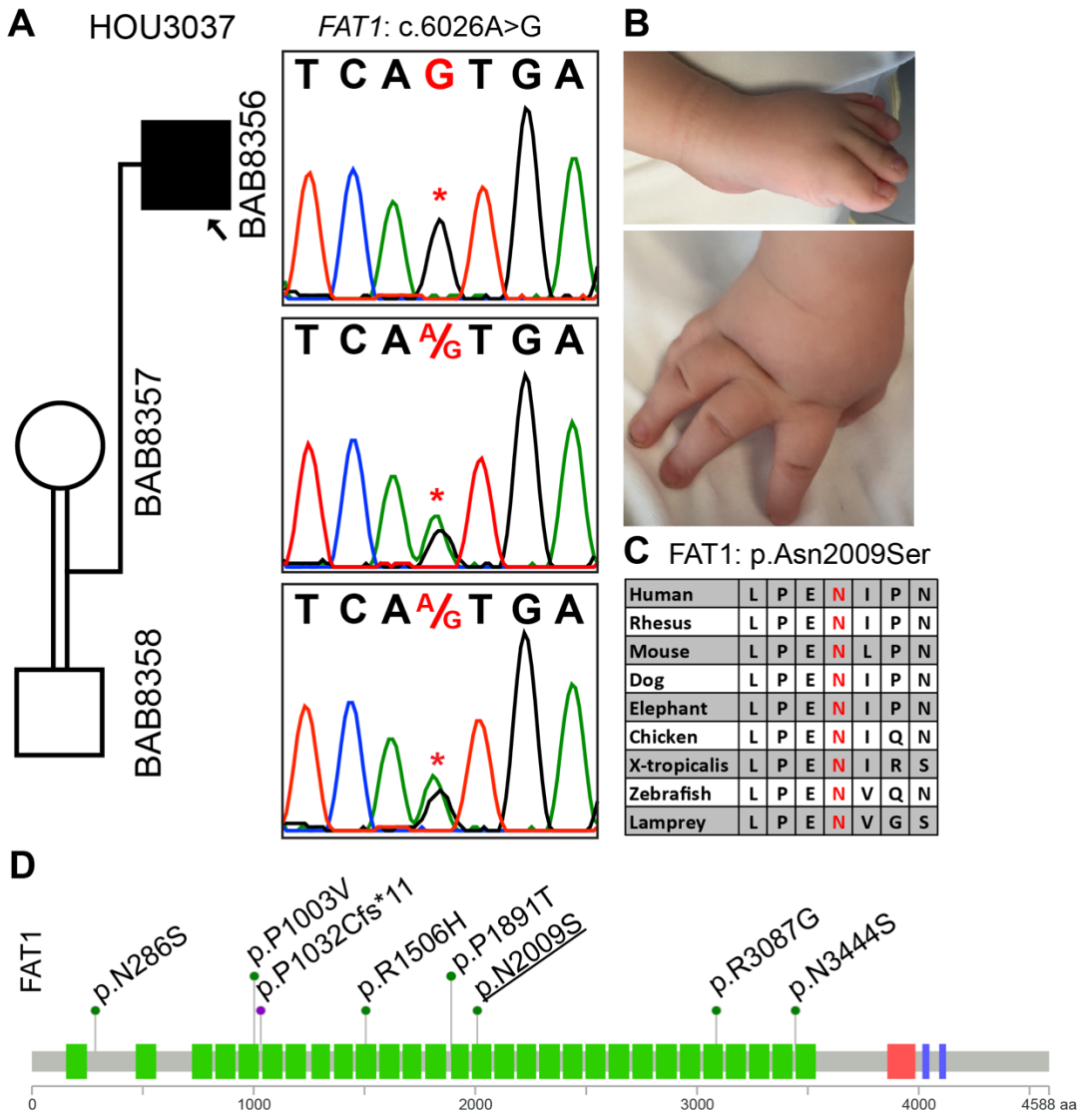

Figure S9: Clinical and genomic studies for homozygous *FAT1* variant in BAB8356. (A) Family HOU3037 pedigree and segregation of the variant c.6026A>G, consistent with autosomal recessive inheritance pattern. (B) Photographs of the hand and feet showing the contractures in fingers and toes. (C) Sequence alignment of human FAT1 in other species. N2009 is a conserved residue across all vertebrates. (D) Protein domains of FAT1 and localization of the identified mutations marked with small circles in Facioscapulohumeral Muscular Dystrophy and glomerulotubular nephropathy. Purple filled circle indicates the frameshift mutation and green filled circles point missense mutations. The variant identified in our case is underlined to distinguish.

Table S2: Molecular summary of the putative pathogenic Copy Number Variants (CNVs) cohort			
Proband	**CNV coordinates**	**CNV type**	**Size**
BAB7128	chr5:129673070-136365890	Deletion	6.6 Mb
BAB8145	chr10:58374373-67805420	Deletion	9.4 Mb
	chr11:90798107-91499657	Deletion	0.7 Mb
	chr11:92950818-100534639	Deletion	7.5 Mb
BAB9312	chr18:21901302-43716565	Duplication	21.8 Mb
	chr18:66350129-78002264	Deletion	11.6 Mb

Table S4: Patients diagnosed with Reanalysis of ES data and Expansion to additional family members				
Proband	**Gene**	**Nucleotide;Protein**	**Zygosity**	**Contributing factors to diagnosis**
BAB3928	*TNNT3*	c.163C>T;p.Arg55Cys	Htz	DNMfinder and literature update
BAB3941	*MFN2*	c.526G>A;p.Gly176Ser	Hmz	Literature update
BAB3944	*FGFRL1*	c.124C>T;p.Arg42Trp	Hmz	Literature update
BAB5192	*TMEM214*	c.764G>A;p.Arg255Gln	Hmz	Literature update
BAB6807 / BAB6808	*COL6A3*	c.619C>T;p.Gln207*	Hmz	Literature update
	ADNP	c.775A>C;p.Asn259His	Hmz	
	ABCA7	c.5092C>T;p.Arg1698Trp	Hmz	
BAB7079	*PLEC*	c.8813C>T;p.Thr2938Met c.6523A>G;p.Lys2175Glu	Comp Htz	Trio expansion
BAB7084	*SYNE1*	c.2839G>A;p.Glu947Lys c.21164A>G;p.Lys7055Arg	Comp Htz	Trio expansion and Literature update
BAB7128	Copy Number Variant			Trio expansion and HMZDelFinder
BAB7308	*SYT2*	c.1081G>C;p.Asp361His	Htz	Trio expansion and DNMfinder

Hmz: Homozygous, Htz: heterozygous, Comp Htz: Compound Heterozygous.
Headings and column titles are bolded, gene names are italicized.

References

1. Alazami, A.M., Kentab, A.Y., Faqeih, E., Mohamed, J.Y., Alkhalidi, H., Hijazi, H., and Alkuraya, F.S. (2015). A novel syndrome of Klippel-Feil anomaly, myopathy, and characteristic facies is linked to a null mutation in *MYO18B*. J Med Genet 52, 400-404.

2. Malfatti, E., Bohm, J., Lacene, E., Beuvin, M., Romero, N.B., and Laporte, J. (2015). A Premature Stop Codon in *MYO18B* is Associated with Severe Nemaline Myopathy with Cardiomyopathy. J Neuromuscul Dis 2, 219-227.

3. Tumiene, B., Voisin, N., Preiksaitiene, E., Petroska, D., Grikiniene, J., Samaitiene, R., Utkus, A., Reymond, A., and Kucinskas, V. (2017). Inflammatory myopathy in a patient with Aicardi-Goutieres syndrome. European journal of medical genetics 60, 154-158.

4. Dlamini, N., Josifova, D.J., Paine, S.M., Wraige, E., Pitt, M., Murphy, A.J., King, A., Buk, S., Smith, F., Abbs, S., et al. (2013). Clinical and neuropathological features of X-linked spinal muscular atrophy (SMAX2) associated with a novel mutation in the *UBA1* gene. Neuromuscular disorders : NMD 23, 391-398.

5. North, K.N., and Ryan, M.M. (1993). Nemaline Myopathy. In GeneReviews((R)), M.P. Adam, H.H. Ardinger, R.A. Pagon, S.E. Wallace, L.J.H. Bean, K. Stephens, andA. Amemiya, eds. Seattle (WA), University of Washington, Seattle

6. Tolmie, J.L., Shillito, P., Hughes-Benzie, R., and Stephenson, J.B. (1995). The Aicardi-Goutieres syndrome (familial, early onset encephalopathy with calcifications of the basal ganglia and chronic cerebrospinal fluid lymphocytosis). Journal of medical genetics 32, 881-884.

7. Bohm, J., Vasli, N., Malfatti, E., Le Gras, S., Feger, C., Jost, B., Monnier, N., Brocard, J., Karasoy, H., Gerard, M., et al. (2013). An integrated diagnosis strategy for congenital myopathies. PLoS One 8, e67527.

8. Bower, N.I., and Johnston, I.A. (2010). Discovery and characterization of nutritionally regulated genes associated with muscle growth in Atlantic salmon. Physiol Genomics 42A, 114-130.

9. Azakir, B.A., Di Fulvio, S., Therrien, C., and Sinnreich, M. (2010). Dysferlin interacts with tubulin and microtubules in mouse skeletal muscle. PLoS One 5, e10122.

10. Schellhaus, A.K., Moreno-Andres, D., Chugh, M., Yokoyama, H., Moschopoulou, A., De, S., Bono, F., Hipp, K., Schaffer, E., and Antonin, W. (2017). Developmentally Regulated GTP binding protein 1 (DRG1) controls microtubule dynamics. Sci Rep 7, 9996.

11. Granot-Hershkovitz, E., Raas-Rothschild, A., Frumkin, A., Granot, D., Silverstein, S., and Abeliovich, D. (2011). Complex chromosomal rearrangement in a girl with psychomotor-retardation and a de novo inversion: inv(2)(p15;q24.2). Am J Med Genet A 155A, 1825-1832.

12. Avirneni-Vadlamudi, U., Galindo, K.A., Endicott, T.R., Paulson, V., Cameron, S., and Galindo, R.L. (2012). Drosophila and mammalian models uncover a role for the myoblast fusion gene *TANC1* in rhabdomyosarcoma. J Clin Invest 122, 403-407.

13. Agrawal, P.B., Pierson, C.R., Joshi, M., Liu, X., Ravenscroft, G., Moghadaszadeh, B., Talabere, T., Viola, M., Swanson, L.C., Haliloglu, G., et al. (2014). SPEG interacts with myotubularin, and its deficiency causes centronuclear myopathy with dilated cardiomyopathy. Am J Hum Genet 95, 218-226.

14. Wang, H., Castiglioni, C., Kacar Bayram, A., Fattori, F., Pekuz, S., Araneda, D., Per, H., Erazo, R., Gumus, H., Zorludemir, S., et al. (2017). Insights from genotype-phenotype correlations by novel *SPEG* mutations causing centronuclear myopathy. Neuromuscul Disord 27, 836-842.

15. Agarkova, I., and Perriard, J.C. (2005). The M-band: an elastic web that crosslinks thick filaments in the center of the sarcomere. Trends Cell Biol 15, 477-485.

16. Schoenauer, R., Lange, S., Hirschy, A., Ehler, E., Perriard, J.C., and Agarkova, I. (2008). Myomesin 3, a novel structural component of the M-band in striated muscle. J Mol Biol 376, 338-351.

17. Lange, S., Agarkova, I., Perriard, J.C., and Ehler, E. (2005). The sarcomeric M-band during development and in disease. J Muscle Res Cell Motil 26, 375-379.

18. Schoenauer, R., Bertoncini, P., Machaidze, G., Aebi, U., Perriard, J.C., Hegner, M., and Agarkova, I. (2005). Myomesin is a molecular spring with adaptable elasticity. J Mol Biol 349, 367-379.

19. Li, H., Bielas, S.L., Zaki, M.S., Ismail, S., Farfara, D., Um, K., Rosti, R.O., Scott, E.C., Tu, S., Chi, N.C., et al. (2016). Biallelic Mutations in Citron Kinase Link Mitotic Cytokinesis to Human Primary Microcephaly. Am J Hum Genet 99, 501-510.

20. Shaheen, R., Hashem, A., Abdel-Salam, G.M., Al-Fadhli, F., Ewida, N., and Alkuraya, F.S. (2016). Mutations in *CIT*, encoding citron rho-interacting serine/threonine kinase, cause severe primary microcephaly in humans. Hum Genet 135, 1191-1197.

21. Basit, S., Al-Harbi, K.M., Alhijji, S.A., Albalawi, A.M., Alharby, E., Eldardear, A., and Samman, M.I. (2016). *CIT*, a gene involved in neurogenic cytokinesis, is mutated in human primary microcephaly. Hum Genet 135, 1199-1207.

22. Angius, A., Uva, P., Buers, I., Oppo, M., Puddu, A., Onano, S., Persico, I., Loi, A., Marcia, L., Hohne, W., et al. (2016). Bi-allelic Mutations in *KLHL7* Cause a Crisponi/CISS1-like Phenotype Associated with Early-Onset Retinitis Pigmentosa. Am J Hum Genet 99, 236-245.

23. Bruel, A.L., Bigoni, S., Kennedy, J., Whiteford, M., Buxton, C., Parmeggiani, G., Wherlock, M., Woodward, G., Greenslade, M., Williams, M., et al. (2017). Expanding the clinical spectrum of recessive truncating mutations of *KLHL7* to a Bohring-Opitz-like phenotype. J Med Genet 54, 830-835.

24. Thompson, A.A., and Nguyen, L.T. (2000). Amegakaryocytic thrombocytopenia and radio-ulnar synostosis are associated with *HOXA11* mutation. Nat Genet 26, 397-398.

25. Arora, P.D., Di Gregorio, M., He, P., and McCulloch, C.A. (2017). TRPV4 mediates the Ca(2+) influx required for the interaction between flightless-1 and non-muscle myosin, and collagen remodeling. J Cell Sci 130, 2196-2208.

26. Naganawa, Y., and Hirata, H. (2011). Developmental transition of touch response from slow muscle-mediated coilings to fast muscle-mediated burst swimming in zebrafish. Dev Biol 355, 194-204.

27. Campbell, H.D., Fountain, S., McLennan, I.S., Berven, L.A., Crouch, M.F., Davy, D.A., Hooper, J.A., Waterford, K., Chen, K.S., Lupski, J.R., et al. (2002). Fliih, a gelsolin-related cytoskeletal regulator essential for early mammalian embryonic development. Mol Cell Biol 22, 3518-3526.

28. Malfatti, E., Barnerias, C., Hedberg-Oldfors, C., Gitiaux, C., Benezit, A., Oldfors, A., Carlier, R.Y., Quijano-Roy, S., and Romero, N.B. (2016). A novel neuromuscular form

of glycogen storage disease type IV with arthrogryposis, spinal stiffness and rare polyglucosan bodies in muscle. Neuromuscul Disord 26, 681-687.

29. Yuan, B., Pehlivan, D., Karaca, E., Patel, N., Charng, W.L., Gambin, T., Gonzaga-Jauregui, C., Sutton, V.R., Yesil, G., Bozdogan, S.T., et al. (2015). Global transcriptional disturbances underlie Cornelia de Lange syndrome and related phenotypes. J Clin Invest 125, 636-651.

30. Alazami, A.M., Patel, N., Shamseldin, H.E., Anazi, S., Al-Dosari, M.S., Alzahrani, F., Hijazi, H., Alshammari, M., Aldahmesh, M.A., Salih, M.A., et al. (2015). Accelerating novel candidate gene discovery in neurogenetic disorders via whole-exome sequencing of prescreened multiplex consanguineous families. Cell Rep 10, 148-161.

31. Herrera, F.J., Yamaguchi, T., Roelink, H., and Tjian, R. (2014). Core promoter factor TAF9B regulates neuronal gene expression. Elife 3, e02559.

32. Rymen, D., Winter, J., Van Hasselt, P.M., Jaeken, J., Kasapkara, C., Gokcay, G., Haijes, H., Goyens, P., Tokatli, A., Thiel, C., et al. (2015). Key features and clinical variability of *COG6*-CDG. Mol Genet Metab 116, 163-170.

33. Soutourina, J. (2018). Transcription regulation by the Mediator complex. Nat Rev Mol Cell Biol 19, 262-274.

34. Lee, M.P., Tanabe, O., Shi, L., Jearawiriyapaisarn, N., Lucas, D., and Engel, J.D. (2017). The orphan nuclear receptor TR4 regulates erythroid cell proliferation and maturation. Blood 130, 2537-2547.

35. Eldomery, M.K., Coban-Akdemir, Z., Harel, T., Rosenfeld, J.A., Gambin, T., Stray-Pedersen, A., Kury, S., Mercier, S., Lessel, D., Denecke, J., et al. (2017). Lessons learned from additional research analyses of unsolved clinical exome cases. Genome Med 9, 26.

36. Herrmann, D.N., Horvath, R., Sowden, J.E., Gonzalez, M., Sanchez-Mejias, A., Guan, Z., Whittaker, R.G., Almodovar, J.L., Lane, M., Bansagi, B., et al. (2014). Synaptotagmin 2 mutations cause an autosomal-dominant form of lambert-eaton myasthenic syndrome and nonprogressive motor neuropathy. Am J Hum Genet 95, 332-339.

37. Pang, Z.P., Melicoff, E., Padgett, D., Liu, Y., Teich, A.F., Dickey, B.F., Lin, W., Adachi, R., and Sudhof, T.C. (2006). Synaptotagmin-2 is essential for survival and contributes to Ca2+ triggering of neurotransmitter release in central and neuromuscular synapses. J Neurosci 26, 13493-13504.

38. Tejero, R., Lopez-Manzaneda, M., Arumugam, S., and Tabares, L. (2016). Synaptotagmin-2, and -1, linked to neurotransmission impairment and vulnerability in Spinal Muscular Atrophy. Hum Mol Genet 25, 4703-4716.